Investigating the effects of the amyloid beta interacting peptide (AIP) on Aβ43 in *Drosophila melanogaster*

Isabel M. Sarty

Integrated Program in Neuroscience

McGill University
Montreal, QC
June 2023

A thesis submitted to McGill University in partial fulfillment of the requirements of the degree of

Master of Science

TABLE OF CONTENTS

ABSTRACT

As the leading cause of dementia, Alzheimer's disease (AD) prevalence will continue to rise with the aging global population. One of the neuropathological hallmarks of AD is extracellular plaques in the brain parenchyma, composed mainly of amyloid beta (Aβ) peptides. Aβ peptides are also involved in the pathology of cerebral amyloid angiopathy (CAA), a highly prevalent disease among AD patients. Although two disease modifying treatments have recently been FDA-approved for AD, controversy surrounding the efficacy, cost, and safety profiles of these passive immunotherapies emphasize the imminent need for novel therapeutic intervention strategies. The Multhaup lab has previously characterized an eight D-amino-acid peptide termed D-AIP and demonstrated its ability *in vitro* and *in vivo* to interact with low-order oligomers of Aβ42 (42 amino-acid peptide), attenuate its toxicity, and disrupt its sheet-to-sheet packing – consequently blocking Aβ fibril formation. While D-AIP was shown to interact with Aβ42, its ability to target other Aβ species has not yet been investigated.

The current study sought to investigate if D-AIP targets Aβ43 (43 amino-acid peptide) longitudinally *in vivo* using a transgenic *Drosophila melanogaster* model. Only one additional threonine residue on the C-terminus longer than Aβ42, Aβ43 is present in both AD and CAA pathologies and has been found to induce aggregation and toxicity of other Aβ peptides – such as the typically innocuous Aβ40 peptide, which is the prominent Aβ peptide in CAA deposits. In this study, we first characterized a transgenic *Drosophila* model with eye-directed expression of human Aβ43, where Aβ43 expression induced toxic eye morphology. Using these transgenic *Drosophila*, we conducted a longitudinal study to assess if D-AIP administration through food supplementation would attenuate Aβ43-induced eye toxicity. In our study, D-AIP successfully reduced Aβ43-induced toxicity throughout the entirety of a 28-day treatment period, with no sex-specific effects.

D-AIP was also confirmed to be protease-resistant and non-toxic over a 28-day treatment period. This study also reproduced results of our previous study by Zhong et al. (2019) in transgenic *Drosophila melanogaster* with eye-directed expression Aβ42, where we found that Aβ42-induced toxicity was not attenuated beyond 5 days post-eclosion.

Together, as D-AIP was found to target two key Aβ peptides heavily involved in the pathology of both AD and CAA, the results of this study suggest that D-AIP presents as a promising therapeutic candidate to prevent or delay the progression of AD and/or CAA. In future studies, it would be valuable to study the effect of D-AIP on Aβ43 seeding in transgenic *Drosophila* models of mixed Aβ43 and Aβ40 expression, and in more complex rodent models of AD and CAA pathologies – ultimately hoping to lead towards an eventual clinical impact.

ABRÉGÉ

La maladie d'Alzheimer (MA) est la cause principale de démence et sa prévalence continuera d'augmenter avec le vieillissement de la population mondiale. Les plaques extracellulaires dans le parenchyme cérébral, composées principalement de peptides bêta-amyloïdes (Aβ), constituent l'une des caractéristiques neuropathologiques de la MA. Les peptides Aβ sont également impliqués dans la pathologie de l'angiopathie amyloïde cérébrale (AAC), une maladie très répandue chez les patients souffrant de la MA. Même si deux traitements pour modifier la maladie ont récemment été approuvés par la FDA pour la MA, la controverse entourant l'efficacité, le coût et les profils de d'innocuité de ces immunothérapies passives met en évidence le besoin imminent de nouvelles stratégies d'intervention thérapeutique. Le laboratoire Multhaup a précédemment caractérisé un peptide de huit D-amino-acides appelé D-AIP et a démontré sa capacité *in vitro* et *in vivo* à interagir avec des oligomères d'ordre inférieur d'Aβ42 (peptide de 42 amino-acides), à atténuer sa toxicité et à perturber son empilement de feuillet à feuillet - bloquant ainsi la formation de fibrilles d'Aβ. Bien qu'il ait été démontré que le D-AIP interagit avec l'Aβ42, sa capacité à agir sur d'autres espèces d'Aβ est encore à découvrir.

La présente étude a visé à déterminer si le D-AIP cible l'Aβ43 (peptide de 43 amino-acides) longitudinalement in vivo en utilisant un modèle transgénique de *drosophile melanogaster*. Avec seulement un résidu thréonine de plus que l'Aβ42 à l'extrémité C-terminale, l'Aβ43 est présent dans les pathologies de la MA et de la AAC et induit l'agrégation et la toxicité d'autres peptides Aβ - comme le peptide Aβ40, typiquement bénin, qui est le peptide Aβ le plus important dans les dépôts de l'AAC. Dans cette étude, nous avons d'abord caractérisé un modèle de *drosophile* transgénique avec une expression de Aβ43 humain dirigée vers l'œil, où l'expression de Aβ43 a induit une morphologie oculaire toxique. En utilisant ces *drosophiles* transgéniques, nous avons

mené une étude longitudinale pour évaluer si l'administration de D-AIP par le biais d'une supplémentation alimentaire atténuerait la toxicité oculaire induite par l'Aβ43. Dans notre étude, le D-AIP a réussi à réduire la toxicité induite par l'Aβ43 pendant la totalité d'une période de traitement de 28 jours, sans effets spécifiques au sexe. Le D-AIP a également été confirmé comme résistant aux protéases et non toxique sur une période de traitement de 28 jours. Cette étude a également reproduit les résultats de notre étude précédente de Zhong et al. (2019) chez la *drosophile melanogaster* transgénique à expression oculaire Aβ42, où s'est trouvée la toxicité induite par Aβ42 n'a pas été atténuée au-delà de 5 jours après l'éclosion.

Étant donné que le D-AIP cible deux peptides Aβ principaux fortement impliqués dans la pathologie de la MA et de la AAC, les résultats de cette étude suggèrent que le D-AIP est un candidat thérapeutique prometteur pour prévenir ou ralentir la progression de la MA et/ou de l'AAC. Dans des futures études, il serait intéressant d'étudier l'effet du D-AIP sur l'Aβ43 comme un modèle permettant le dépôt de Aβ dans des modèles de *drosophiles* transgéniques présentant une expression mixte de l'Aβ43 et de l'Aβ40, ainsi que dans des modèles de rongeurs plus complexes des pathologies de la MA et de la AAC, dans l'espoir de réaliser un éventuel impact clinique.

ACKNOWLEDGEMENTS

I would like to thank my supervisor, Dr. Gerhard Multhaup, for welcoming me into his lab and providing mentorship throughout my time here. His passion for the progression of Alzheimer Disease research, his philosophy of teaching diligence, attentiveness, and thoroughness in science, and his extensive knowledge not only inspired me, but allowed me to significantly grow as a young researcher in his laboratory. In pursuing my thesis under Dr. Multhaup's supervision, I gained technical and problem-solving skills which increased my confidence in working independently, while also learning when to ask for help and guidance from others.

Additionally, I would like to thank all current and previous members of the Multhaup lab. Thank you to Dr. Adeola Shobo for your guidance, advice, and support throughout my thesis studies. Your enthusiasm for research, and the D-AIP project in particular, was motivating throughout my experiments. Thank you to Dr. Mark Hancock for performing MALDI experiments for my thesis and guiding me through the analyses – in addition to your advice and help in presentations and writing. Thank you to Dr. Irem Ulku, Hedi Zhou, Fritz Herre, and Robert Kwizera for being great lab members and friends. I am so thankful for our friendship throughout my degree, your support, and the scientific knowledge (and wisdom) that you have shared with me over the last two years. Thank you to previous lab members Lina Walther, for your kindness and bright energy in the lab, and Christelle Sheepers, for training me on *Drosophila* and guiding me when I first arrived at the lab. Outside of the Multhaup lab, I would like to thank Dr. Nicolas Audet for training me in confocal microscopy, allowing me to conduct my thesis experiments.

Thank you to my committee members, Dr. Anne McKinney, and Dr. Yong Rao, for providing their time, insight, and valuable guidance throughout my research. I am also grateful to my IPN mentor, Dr. Pierre Lachapelle, for his support and time.

Thank you to the McGill Swim Team and my coaches, Peter and Sav, for your unwavering support and patience over the last two years. All your belief in my potential as a scientist, swimmer, and human has been incredible. I can truly say that I have experienced the positive impacts of having a full team of people actively cheering me on every day for the last two years, and I feel so lucky.

Lastly, thank you to my family: Diane, Adam, Julia, and my boyfriend, Eric. I could not have made it through last two years without your love and encouragement from Halifax and in Montreal. I am so appreciative for all of you being there (or on the phone) unconditionally throughout my degree, to witness and reassure me during moments of growth, of failures, and of small triumphs. I am eternally grateful for all of you, and I will never forget the time and compassion that you have all given me.

CONTRIBUTION OF AUTHORS

This MSc thesis study was conceived by Dr. Gerhard Multhaup and Dr. Adeola Shobo. The experimental methods were modeled after the PhD thesis of Dr. Yifei (Phoebe) Zhong. I designed the experimental plan of this thesis with the help of Dr. Multhaup and Dr. Shobo, and suggestions from members of the Multhaup Lab and Dr. Mark Hancock. I performed all experiments and analyses (with the exception of MALDI-TOF mass spectrometry) guided by experimental protocols established by Dr. Zhong and Christelle Sheepers. MALDI-TOF mass spectrometry analyses were performed by Dr. Hancock, guided by protocols established by Dr. Shobo.

LIST OF FIGURES

LIST OF ABBREVIATIONS

αCTF: Alpha C-terminal fragment

Acp70A: Accessory gland protein-70A

AD: Alzheimer's disease

AICD: APP intracellular domain

AIP: Aβ-interacting peptide

ANOVA: Analysis of Variance

APP: Amyloid precursor protein

APPL: *Drosophila melanogaster* APP ortholog

Aβ: Amyloid-β

BACE1: β-site APP cleaving enzyme

BBB: Blood-brain barrier

CAA: Cerebral amyloid angiopathy

CD: Circular dichroism

D-AIP: AIP composed of D-amino acids

EDTA: Ethylenediaminetetraacetic acid

FAD: Familial Alzheimer's Disease

FDA: Food and Drug Administration

GdnHCl: Guanidine hydrochloride

GMR: Glass multimer reporter

HCCA: α-Cyano-4-hydroxycinnamic acid

HEPES: 4-(2-hydroxyethyl)-1-piperazineethanesulfonic acid

HRP: Horse-radish peroxidase

L-AIP: AIP composed of L-amino acids

LTP: Long-term potentiation

mAbs: monoclonal antibodies

MALDI-MSI: MALDI mass spectrometry imaging

MALDI-TOF: Matrix-assisted laser desorption/ionization time-of-flight

MCI: Mild cognitive impairment

MSD: Meso Scale Discovery

NMDA: N-methyl-D-aspartate

PBS: Phosphate buffered saline

PCR: Polymerase chain reaction

PSEN1: Presenilin 1

PSEN2: Presenilin 2

S-AIP: Scrambled version of AIP

SAD: Sporadic Alzheimer's Disease

SDS-PAGE: Sodium dodecyl sulfate polyacrylamide gel electrophoresis

SDS: Sodium dodecyl sulfate

SEM: Standard error of the mean

TEM: Transmission electron microscopy

Tris-HCl: Trisaminomethane hydrochloride

UAS: Upstream activating sequence

WT: Wildtype control

1. INTRODUCTION

Alzheimer's disease (AD) is the leading cause of dementia, accounting for 60-80% of all dementia cases, and disproportionally affects females[1]. The disease was first described in the early 1900s by Alois Alzheimer of his patient, Auguste D., who exhibited progressive cognitive impairment – including reduced comprehension and memory, aphasia, hallucinations, disorientation, and paranoia[2,3]. AD significantly decreases patients' lifespans and is a major cause of mortality[4,5]. It progressively impairs cognitive function (such as learning and memory), behaviour, and eventually motor function (affecting speaking, swallowing, and walking)[1]. Ultimately, the cognitive decline due to AD results in a loss of autonomy in those with the disease, leading to their need for full-time care.

As the population ages, the global prevalence of dementia will continue to increase significantly, driving further stress on the financial and emotional toll in patients, caretakers, and family members. Although two recently FDA-approved disease modifying treatments exist to treat AD, their risk-benefit profiles have been questioned due to cost and safety concerns[6,7]. Thus, novel therapeutic strategies are urgently needed to prevent AD and its progression.

1.1. Etiology of AD

AD is characterized by two main neuropathological hallmarks: extracellular plaques and neurofibrillary tangles. Extracellular plaques in the brain parenchyma are accumulations composed mainly of ~4-kDa amyloid beta (Aβ) peptides, while neurofibrillary tangles are intracellular aggregates of hyperphosphorylated tau[8,9]. The neuropathological cascade begins decades prior to the onset of clinical symptoms[9,10] and leads to widespread synaptic disfunction and neuronal death[11].

The majority of AD patients develop Sporadic Alzheimer's Disease (SAD), with clinical symptoms sporadically occurring later in life at 65 years of age or older[12]. This is understood to be a multifactorial disease caused by the interaction of genetic and environmental factors[5,13]. However, between 5-10% of AD patients inherit a rare familial form of AD (FAD) and develop symptoms between the ages of 30 to 50[5,13,14]. FAD is usually attributed to inherited mutations in three principal genes that are related to Aβ processing: the amyloid precursor protein (*APP*, located on chromosome 21), presenilin 1 (*PSEN1*, located on chromosome 14), and presenilin 2 (*PSEN2*, located on chromosome 1); mutations in these genes result in a shift in the metabolism of APP, leading to increased generation and aggregation of toxic Aβ peptides of varying legnths[5,15,16].

1.2. The amyloid hypothesis

The pathological cascade of Alzheimer's Disease is hypothesized to be initiated by changes in Aβ homeostasis[17]. Altered Aβ homeostasis may be caused by increased production and/or decreased clearance of Aβ peptides[11,17,18]. Aβ peptides with different N- and C- truncations are derived from sequential proteolytic cleavages of the Amyloid precursor protein (APP) by secretases[17]. Accumulation of Aβ is proposed to induce tau hyperphosphorylation – and unlike mutations that impact Aβ production, tau mutations alone do not cause AD[5]. Further evidence in support of the amyloid hypothesis arises from the propensity of individuals with Down syndrome to develop early-onset AD, including pathological Aβ plaques, neurofibrillary tangles, and clinical dementia symptoms[19,20]. As the *APP* gene is located on chromosome 21, the duplication of this chromosome in Down Syndrome results in an additional copy of *APP*, resulting in increased Aβ production and subsequent accumulation[19,20].

1.3. APP processing and Aβ production

APP is expressed ubiquitously as a single transmembrane domain protein and is processed by two major pathways: the non-amyloidogenic pathway and the amyloidogenic pathway (**Figure 1**). The predominant non-amyloidogenic pathway prevents the formation of neurotoxic Aβ peptides[21]. APP is cleaved at the plasma membrane within the Aβ domain by α-secretase (between residues 687 and 688), resulting in a C-terminal fragment (αCTF) and the release of the non-toxic large soluble ectodomain sAPPα[15,22-24]. sAPPα has been proposed as an important mediator in neuronal plasticity/survival and neuroprotection against cytotoxicity[22]. αCTF is subsequently cleaved by γ-secretase to yield a 3kDa fragment (P3), and an APP intracellular domain (AICD)[24,25]. The γ-secretase complex consists of four subunits, notably containing one of two presenilin homologues (PSEN1 or PSEN2), which are γ-secretase's crucial catalytic components and impact its subcellular localization[22,26].

Alternatively, APP is processed through the amyloidogenic pathway leading to the generation of Aβ. APP is cleaved by β-secretase (BACE1) at the β-site (between residues 671 and 672), producing βCTF fragments and releasing a large soluble ectodomain sAPPβ[22]. In contrast to sAPPα, sAPPβ has been implicated in neuronal body and axon degeneration[27]. The membrane-associated βCTF undergoes further cleavage by γ-secretase at the C-terminal of the Aβ domain to produce AICD and Aβ peptides of varying lengths (1-XX: e.g., Aβ1-40) which are released extracellularly[11,15,22]. Cleavage of APP by BACE1 also occurs at the β'-site (between residues 681 and 682) to yield β'CTF and produce N-truncated Aβ peptides (11-XX: e.g., Aβ11-40) following γ-secretase cleavage[28].

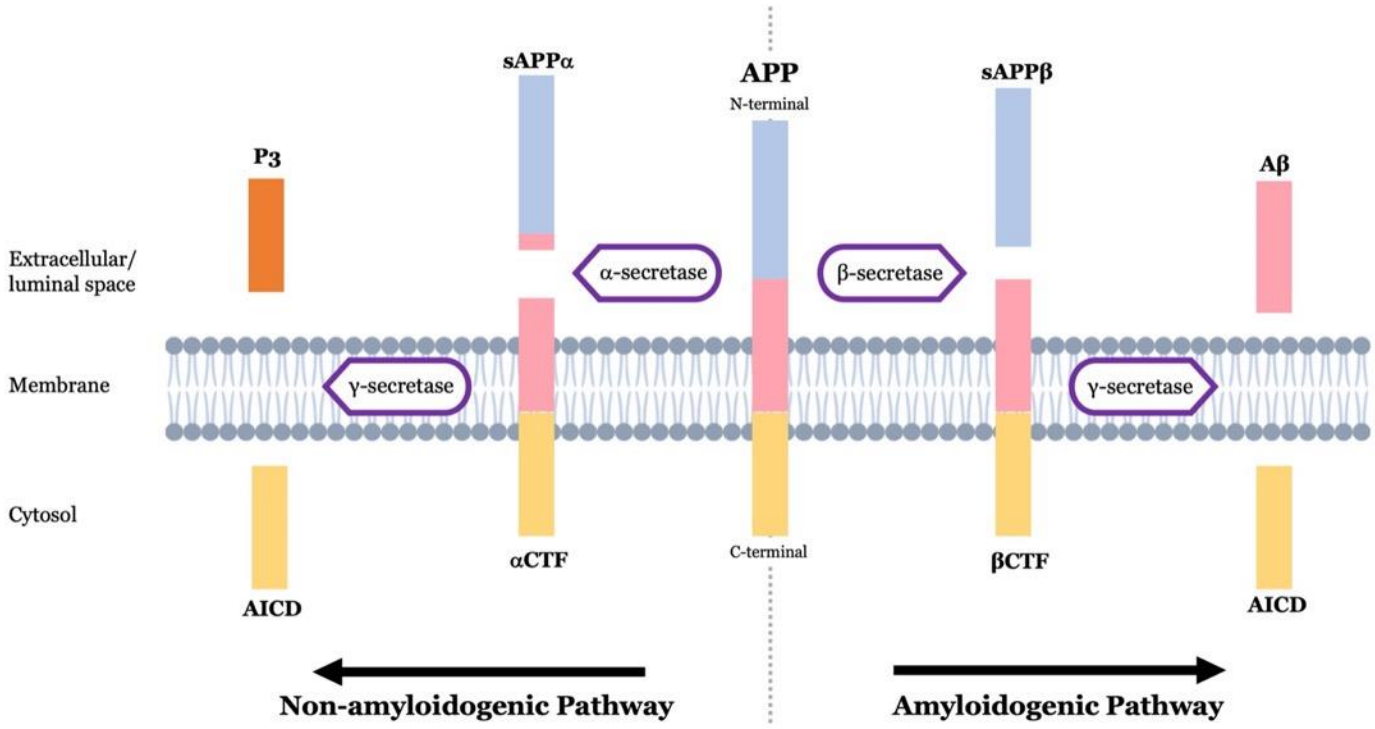

Figure 1. APP proteolysis pathways
The non-amyloidogenic pathway (left) and amyloidogenic pathway (right) of APP proteolysis. On the left: APP is first cleaved by α-secretase to produce sAPPα (blue and pink) and αCTF (pink and yellow), then subsequently cleaved by γ-secretase to generate the non-toxic P3 fragment composed of non-pathogenic Aβ residues such as 17-40 and 17-42 (orange) and AICD (yellow). On the right: APP is first cleaved by β-secretase to produce sAPPβ (blue) and βCTF (pink and yellow), then subsequently cleaved by γ-secretase to generate AICD (yellow) and Aβ peptides of varying lengths associated with AD pathogenesis such as Aβ40, Aβ42, and Aβ43 (pink).

1.4. Cerebral amyloid angiopathy (CAA)

In addition to depositing in the brain parenchyma as plaques, Aβ accumulates into fibrils and deposits on the walls of cerebral vasculature as cerebral amyloid angiopathy (CAA)[29]. CAA is highly prevalent in AD patients; approximately 80% of AD patients also demonstrate CAA pathology and CAA is proposed to contribute synergistically to cognitive decline in AD[29-32]. Given the large prevalence and overlapping pathology between AD and CAA, there has been strong evidence of mechanistic interactions between the two diseases – therefore encouraging the notion that disease-modifying treatment for either AD or CAA may be considered as a treatment for both or mixed pathologies[32].

Impaired perivascular clearance of Aβ (such as Aβ40, Aβ42, Aβ43) from interstitial fluid is a shared pathogenic mechanism in both CAA and AD. The deposition of Aβ in vessel walls in CAA is proposed to interfere with perivascular clearance of Aβ, leading to a self-reinforcing cycle of increased Aβ deposition. CAA-related Aβ deposition results in a loss of vascular smooth muscle cells, leading to decreased vasoactivity, exacerbating AD pathology through reduced Aβ clearance. The accumulation of Aβ and consequent loss of vessel integrity in CAA often leads to brain injuries such as ischemia and hemorrhagic lesions, which range from small cerebral microbleeds to large symptomatic intracerebral hemorrhages[32].

1.5. Aβ forms

Among the differing Aβ isoforms produced by BACE1 and γ-secretase cleavages, Aβ peptides consisting of 40 (Aβ40) and 42 amino acids (Aβ42) are the most prominent[33]. The relative concentration of Aβ42 to Aβ40 is an established biomarker of disease severity/progression and a determinant in the distribution of amyloid pathology (parenchymal or vascular deposition)[33-35]. Aβ42 is considered to be the main pathogenic form of Aβ; it has been shown to lead to synaptic

damage and neurodegeneration, and its hydrophobicity and increased propensity to aggregate gives rise to oligomeric intermediates and insoluble fibrils deposited in plaques[9,29,36]. Aβ42 is the major species deposited in senile plaques of AD, whereas Aβ40 preferentially accumulates in the cerebrovasculature – however, although at lower levels, Aβ42 and Aβ40 are present in vascular Aβ deposits and senile plaques, respectively[32,33,37-39]. While Aβ40 is produced at higher levels than Aβ42, it is significantly less prone to aggregation and less neurotoxic than the Aβ42 peptide[40]. The involvement of the kinetically soluble Aβ40 in amyloid pathology of AD and CAA is proposed to be nucleation-dependent, where Aβ40 is seeded by small amounts of kinetically insoluble Aβ peptides[40-42].

Aβ43 has been proposed as a primary nucleator of Aβ aggregates in AD[43], inducing Aβ deposition in initial pathological stages of AD and CAA[42-45]. Aβ43 is extended by a single hydrophilic threonine residue (Thr43) relative to Aβ42, which has been found to significantly affect the structure and aggregation properties of Aβ43[43]. For example, compared to the C-termini of Aβ42 and Aβ40, Thr43 favours direct contact with the protofibril surface and Thr43 increases the rate and extent of protofibril formation[43]. Although total levels of Aβ43 in human AD brains are low compared to Aβ42 and Aβ40[46], Aβ43 is highly aggregative and neurotoxic[17,31,40,41,44,47,48], is present in AD plaque cores at higher levels than Aβ40[48], and is also present in vascular Aβ deposits[34]. Taken together, Aβ43 presents as a significant potential therapeutic target.

1.6. Aβ aggregation and toxicity

Soluble Aβ monomers can self-assemble into heterogenous intermediate oligomers, protofibrils, and finally, insoluble fibrils through intermolecular β-sheet packing, forming cross-β sheet structures[49,50]. The accumulation of Aβ is a primary and secondary nucleation-dependent two-step process, where a small Aβ aggregate (nucleus) acts as a misfolded protein template,

facilitating subsequent accelerated growth of an aggregate through the addition of soluble monomers[49]. Primary nucleation is the initialization process of amyloid aggregation. In this process, nuclei are formed from monomeric Aβ at a rate that is dependent on the concentration of monomers and independent of existing fibril concentration[51,52]. Alternatively, the formation of a nucleus may also be catalyzed on the surface of existing Aβ aggregates in a process termed secondary nucleation[51,53]. The rapid rate of Aβ aggregation through secondary nucleation is influenced by the dynamic growth and fragmentation of existing Aβ fibrils through a process known as seeding[49]. Aβ fibril fragmentation produces seed material which acts as misfolded protein template (or nuclei) and recruit soluble Aβ monomers – therefore bypassing the energetically unfavourable and rate-determining step of primary nucleation and proceeding with accelerated accumulation of Aβ[53]. This process increases the number of replicative entities, ensuing fibril fragmentation, elongation, and propagation of Aβ[49].

Derived from both primary and secondary nucleation pathways, soluble, pre-fibrillar oligomeric forms of Aβ are considered the most neurotoxic form of Aβ. Soluble Aβ oligomers have been shown to impair long-term potentiation (LTP) and dendritic spine structure in the hippocampus and are correlated with the cognitive deficits and disease symptoms of AD[5,11,42,54,55].

1.7. Therapeutics for AD

Despite decades of extensive research and new discoveries made regarding the pathogenesis of AD, there is yet to be a cure for the disease. Between the two categories of therapeutics for AD (symptomatic or disease-modifying), current clinical treatment for AD is limited to treating symptoms, while disease-modifying treatments have not experienced much success in clinical practice[56,57]. The Food and Drug Administration (FDA) approved symptomatic treatments for AD at present include acetylcholinesterase inhibitors (donepezil, galantamine,

rivastigmine) and N-methyl-D-aspartate (NMDA) receptor antagonists (memantine) to increase the concentration of the neurotransmitter acetylcholine, and inhibit NMDA receptor-induced excitotoxicity, respectively[14,57,58]. Symptomatic treatments are aimed to improve the cognitive impairment and neuropsychiatric symptoms in patients with AD, however they do not address or modify the biological underpinnings of AD that result in neuronal death. Approximately 20 years prior to the onset of clinical dementia symptoms, the process of Aβ accumulation begins[9,10,57]. This asymptomatic period (classified as the pre-clinical AD stage) complicates the efficacy of disease-modifying AD treatment at the onset of clinical symptoms in patients (i.e., mild cognitive impairment stage of AD and eventual dementia).

1.8. Disease-modifying treatments for AD

There has been a shift in AD research towards novel disease modifying treatments and therapeutic targets to reduce the risk and/or prevent the clinical manifestation of AD. However, most disease-modifying therapeutics have either not progressed to, or have failed, phase 3 clinical trials[5,14,17,56,59]. Among the most investigated disease-modifying strategies at present are monoclonal antibodies (mAbs), targeting Aβ in passive immunotherapy to mediate the clearance of Aβ from the brain[6]. After nearly 20 years without any new FDA-approved therapeutics for AD, the FDA recently approved two disease-modifying therapeutics, aducanumab (June 2021) and lecanemab (January 2023)[7,60]. Both therapeutics are mAbs that target Aβ plaques and oligomers[61], intended for the initiation of treatment in patients with mild cognitive impairment (MCI) or mild dementia stage of AD[7,60]. Although encouraging, mAbs have high costs and associated risks of developing vasogenic cerebral edema and cerebral micro-hemorrhages – therefore, their risk-benefit profile has been questioned[6]. There is a common hypothesis that disease-modifying drugs are being delivered to patients too late in the disease process, therefore hindering their efficacy.

This obstacle further emphasizes not only the need for preventative or early intervention treatments, but also the need for affordable and accessible treatments.

1.9. Aβ-interacting peptide (AIP) as a disease-modifying therapeutic candidate

Based on the premise of oligomers being the most neurotoxic form of Aβ, Aβ oligomers are an attractive target for disease-modifying therapeutics. Aβ peptides contain three consecutive repeats of a GxxxG motif that encompasses Aβ residues G25 to G37, which form molecular grooves and notches that facilitate and stabilize sheet-to-sheet stacking of Aβ[62]. The Multhaup lab has previously demonstrated the importance of the central GxxxG motif (containing residue G33) in the inhibition of long-term potentiation by Aβ42, and the oligomerization and toxicity of Aβ42[63,64].

The lab of Dr. Steven Smith and collaborators used the corrugated structure of Aβ peptides to design short peptide inhibitors that disrupt sheet-to-sheet packing and block Aβ fibril formation[62,65]. Our lab (the Multhaup lab) has been investigating the potential of a similar, further developed peptide, as a disease-modifying therapeutic for the early intervention of AD and CAA. This peptide, which we termed the Aβ-interacting peptide (AIP), is an eight amino-acid peptide with a sequence of RGTFEGKF. Our lab has previously characterized AIP and discovered that AIP interacts with low-order Aβ42 oligomers at glycine grooves of the GXXXG motif[66]. We have also demonstrated that AIP attenuates further aggregation of Aβ42 into proto-fibrillar structures and neutralizes the toxicity of Aβ42 oligomers[66].

In organotypic hippocampal slice cultures, AIP reduced Aβ42-induced synaptic spine density loss and rescued LTP[66]. Notably, we used the D-enantiomer of AIP (D-AIP) and characterized it as protease resistant, capable of crossing the invertebrate blood brain barrier (BBB) and showed that it rescued Aβ-induced toxicity in transgenic *Drosophila melanogaster*

expressing human Aβ42 in the eye[66,67]. Typically, D-enantiomers are known to be more resistant to proteolysis and have increased biostability as therapeutics compared to their natural L-enantiomers[68]. In 2015, our lab demonstrated that D-AIP significantly prevented photoreceptor dysfunction and degeneration in 5-day-old (days post-eclosion) transgenic Aβ42 flies; however, the L-enantiomer of AIP (L-AIP) did not demonstrate significant rescue effects[66].

Subsequently in 2019, our lab's longitudinal study using transgenic Aβ42 flies further demonstrated D-AIP's ability to attenuate the toxicity of Aβ42, without impacting survival or locomotor behaviour[67]. In transgenic flies expressing Aβ42 in eye tissue, live confocal imaging was used to evaluate Aβ42-induced toxicity on compound eye morphology. The effect of D-AIP on Aβ42-induced toxicity was assessed on both 5 and 28 days post-eclosion. When flies were bred and raised on D-AIP-supplemented food, Aβ42-induced toxicity was rescued in 5 days post-eclosion female flies. However, toxicity was not rescued in 28 days post-eclosion female flies, or male flies at either 5 or 28 days post-eclosion. Failure of D-AIP to rescue Aβ42-induced toxicity in male flies was likely due to co-localization and interaction of D-AIP with a confounding male-specific sex peptide (Acp70A) in their gut.

In the same study, food supplementation with L-AIP and a scrambled version of AIP (S-AIP) was also investigated[67]. L-AIP was more readily degraded in *Drosophila melanogaster* than D-AIP, while S-AIP showed no attenuation of toxicity or detrimental side effects – demonstrating the increased effectiveness, bioavailability, and specificity of D-AIP.

1.10. *Drosophila melanogaster* as a model for AD

The *Drosophila melanogaster* model is ideal for *in vivo* screening of therapeutics in Alzheimer's disease[23,69]. The adult fly is a complex invertebrate organism that possesses structures that perform equivalent functions of mammalian human organs – including the brain and a

corresponding BBB – allowing for key assessments of a therapeutic's distribution, metabolic stability, and low toxicity[69,70]. The fly's rapid generation time, relatively low cost, and ease of genetic manipulation provide an important preliminary *in vivo* screening model prior to conducting studies in higher organisms such as rodent models[70].

Many *Drosophila* models of AD induce expression of Aβ42 in the compound eye[71]. The notable advantages of eye-expression models are the ease of phenotype detection, and their tolerance to disruptions of basic biological processes of the eye since it is dispensable for survival[71]. Toxicity in the *Drosophila* compound eye presents as a "rough eye" phenotype of varying severity[71]. The eyes of Drosophila are arranged in a honeycomb-like structure, composed of approximately 800 ommatidia[72]. Each ommatidium comprises eight photoreceptor cells and 12 accessory cells, including pigment cells. Expression of toxic transgenes in the eye result in a loss of photoreceptors and/or disruption in their packing. The rough eye phenotype is characterized by abnormalities in this honeycomb-like organization; missing cells disrupt the integrity of the hexagonal lens structure of ommatidia, leading to fused ommatidia, square or misshapen lens facets, and/or general disorganization of ommatidia[72].

Transgenic fly models with eye-specific expression of Aβ43 have rarely been studied compared to Aβ42-expressing fly models, and the toxicity of Aβ43 *in vivo* is not as clear. In 2015, the lab of Dr. Partridge generated transgenic *Drosophila* models of amyloid pathology through either eye-specific or neuron-specific expression of Aβ43[47]. Expression of Aβ43 in the eyes led to the progressive loss of photoreceptor neurons resulting in a rough eye phenotype, while neuron-specific expression of Aβ43 caused altered locomotion and decreased lifespan of the flies[47]; they concluded that Aβ43 peptides are mainly insoluble and highly toxic *in vivo*, though to a milder degree than Aβ42.

2. RATIONALE, AIMS and HYPOTHESIS

Soluble, pre-fibrillar oligomeric forms of Aβ play a major role in the pathogenesis and disease symptoms of AD through impairing LTP and dendritic spine structure in the hippocampus, presenting as a logical therapeutic target for disease-modifying treatment of AD. The Multhaup lab's previous findings that D-AIP targets and neutralizes low-order Aβ42 oligomers both *in vitro* and *in vivo* have been extremely encouraging.

Both AD and CAA pathologies encompass the presence and interaction of Aβ peptides that vary in length (not only Aβ42) – prompting the question if D-AIP targets other Aβ species, such as Aβ43. Considering the proposed role of Aβ43 as a seeding peptide in both AD and CAA, inducing Aβ deposition at initial pathological stages, this thesis seeks to determine if D-AIP can target and rescue Aβ43-induced toxicity *in vivo,* in a longitudinal study using transgenic *Drosophila melanogaster* models as a screening system.

This thesis has two aims. First, we aimed to characterize and quantify the toxicity of the compound eye in transgenic *Drosophila* that express human Aβ43 under an eye-specific promotor. Using live confocal imaging, the gross morphology of transgenic *Drosophila* compound eyes was evaluated and quantified. This was done at two time points (5 and 28 days post-eclosion) to establish a longitudinal phenotypic baseline for Aβ43-induced toxicity in our transgenic *Drosophila* model, prior to performing longitudinal rescue studies at those specific time points.

Aim two longitudinally assessed the ability of D-AIP to target and neutralize Aβ43-induced toxicity in transgenic *Drosophila* through food supplementation. Flies were bred and raised on either D-AIP supplemented food, or regular non-supplemented food as a control. Live confocal imaging was used to assess and quantify the gross morphology/rough eye phenotype of the compound eye, at 5, 14, and 28 days post-eclosion across all treatment groups of each sex. The

uptake and biostability of D-AIP by *Drosophila* was confirmed using matrix-assisted laser desorption/ionization time-of-flight (MALDI-TOF) mass spectrometry. Immunoprecipitation and Western blotting were performed across treatment groups of each sex to assess if D-AIP has an effect on soluble and insoluble levels of Aβ43. A survival assay was also conducted to evaluate any effects of D-AIP consumption on the longevity of *Drosophila*.

This experiment utilized three different transgenic fly models under eye-specific promotors to express either human Aβ43, Aβ42, or no human transgene (i.e., wildtype control, WT). Human Aβ42-expressing transgenic flies served as a control as an established model of Aβ42-induced eye toxicity. Additionally, Aβ42-experessing *Drosophila* were utilized in this study as a control on D-AIP's effect on Aβ42-induced toxicity in *Drosophila melanogaster*[66,67]. Sex-specific outcomes of D-AIP administration were investigated across experiments in this study.

We hypothesized that D-AIP would successfully target and neutralize the toxicity of Aβ43 oligomers *in vivo*, using transgenic *Drosophila melanogaster* as a model. Recent preliminary *in vitro* experiments from our lab have used transmission electron microscopy (TEM), circular dichroism (CD) spectroscopy, and MALDI-TOF mass spectrometry to investigate if D-AIP interacts with synthetic Aβ43. These recent experiments have successfully demonstrated that *in vitro* incubation of synthetic Aβ43 peptides with D-AIP results in interactions between D-AIP and soluble low-order Aβ43 oligomers – providing convincing foundation to move forward with *in vivo* experiments using *Drosophila melanogaster*. Our hypothesis was grounded in these *in vitro* results, along with the previously documented biostability of D-AIP *in vivo* (using *Drosophila melanogaster*[67] and wildtype mice[73]) and its ability to cross the invertebrate BBB.

Together, the results from our study on D-AIP's longitudinal effect on *Drosophila* eye toxicity, D-AIP's effect on *Drosophila* survival, and D-AIP's effect on Aβ levels in *Drosophila*

will advance our understanding of D-AIP's potential as a therapeutic agent. Building on our previous findings that D-AIP attenuates Aβ42-induced toxicity, if D-AIP successfully attenuates Aβ43-induced toxicity in *Drosophila melanogaster*, this study will demonstrate the utility of D-AIP to target multiple toxic Aβ species associated with both AD and CAA.

3. MATERIALS and METHODS

3.1. Transgenic *Drosophila melanogaster*

Transgenic *Drosophila melanogaster* achieved tissue-specific expression of a transgene through the GAL4/UAS binary expression system, which was first described by Brand and Perrimon in 1993[74]. The GAL4/UAS system accomplishes tissue-specific expression of a transgene in the progeny (F1) of a cross between two parental fly strains. In one parental strain, yeast transcription factor GAL4 is fused to a tissue specific promotor. In the other parental strain, the yeast galactose upstream activator sequence (GAL4 response element, UAS) is fused upstream of an inserted transgene. When a genetic cross is performed, the transcriptional activator GAL4 binds to UAS, inducing tissue-specific expression of the transgene of interest in the F1 generation. To attain an eye-specific expression of a given transgene in this study, a *GMR*-GAL4 driver line was used, where GAL4 is linked to the promotor glass multimer reporter (*GMR*).

UAS-Aβ43 flies were generated by the lab of Dr. Linda Partridge at University College London[47]. UAS-Aβ42 flies were generated as previously described[63]. Both UAS-Aβ43 and UAS-Aβ42 flies were crossed with *GMR*-GAL4 flies (Bloomington Drosophila Stock Center) to achieve eye-specific expression of Aβ peptide. Canton S flies (Bloomington Drosophila Stock Center) were crossed with *GMR*-GAL4 flies to create a driver line control.

All experimental fly lines were raised in a 25°C incubator (Tritech) with 12hr light/dark cycle and 50% humidity. For the toxicity assay in aim one, all flies were bred and raised on Jazz-Mix *Drosophila* fly food, prepared according to the manufacturer's instructions (Thermo Fisher Scientific Inc.).

3.2. DNA extraction and polymerase chain reaction (PCR) to confirm presence of human Aβ43 transgene

After receiving UAS-Aβ43 flies from the lab of Dr. Linda Partridge, DNA extraction and subsequent PCR were performed to confirm the presence of the human Aβ43 transgene in their genome. Fifty UAS-Aβ43 flies were anesthetized with CO_2, collected, and snap-frozen using liquid nitrogen. Briefly, flies were homogenized in 400µL of lysis buffer (0.1 M Tris-HCl (pH 9), 0.1 M EDTA and 1 % SDS) and incubated for 30 minutes at 70°C. After adding 56µL of potassium acetate (8 M), the sample was left on ice for 30 minutes. The sample was then centrifuged at 12 000 rpm and 4°C for 15 minutes and the resulting supernatant was collected. Cold isopropanol was added to the supernatant, and the supernatant was centrifuged again. Next, 70% ethanol was added, followed by centrifugation for 10 minutes at 12 000 rpm and 4°C. The supernatant was discarded, and the dried pellet was resuspended in 100µL of deionized Milli-Q® water.

The extracted DNA was then used in PCR experiments to amplify the transgene. Primers were designed to encompass the transgene, targeting the start of the signal peptide sequence of *Drosophila* Hedgehog (*hh*) (for extracellular release of Aβ43) and the end of the proceeding DNA sequence encoding human Aβ43. The resulting DNA fragments from PCR were separated on a 2% agarose gel, where the DNA fragment band was then excised from the gel, extracted, and purified using a NucleoSpin® Gel and PCR Cleanup Kit (Macherey Nagel, Germany). The DNA sample was then sent to the McGill University and Génome Québec Innovation Centre (Montréal, Canada) for Sanger sequencing to confirm the presence of Aβ43.

3.3. Live confocal imaging

Longitudinal confocal imaging of live flies was performed at the Imaging & Molecular Biology Platform (Department of Pharmacology & Therapeutics, McGill Life Sciences Complex),

as previously described[67,75]. Briefly, flies of all genotypes, aged either 5 or 28 days, were immobilized sagittally in 35mm plates half filled with 2% low melting point agarose (Fisher Scientific) at 45°C. Half of the body and head was embedded in the agarose, with one eye exposed. Plates were placed on ice to solidify the agarose, and the flies were covered in ice cold water for anesthetization and cornea neutralization. Eyes of the immobilized flies were imaged using a TCS SP8 confocal microscope (Leica; HCX IRAPO L 25X/0.95NA water-immersion objective; green laser [552] set at 12 % power). Visualization of ommatidia with fluorescence microscopy is possible due to the autofluorescence of outer photoreceptors and pigment cells[72]. After imaging, the embedded flies were retrieved from the agarose using forceps, dried on Kimwipes (Kimberly-Clark), and placed back into their initial tubes. Tubes were placed on their side overnight to prevent flies from sticking to the food and to allow time to recover. Acquired z-stacks were combined using the Leica Application Suite X (LAS X) software (3.7.5.24914, Leica Microsystems). Relative eye toxicity ("rough eye" phenotype) for each fly was defined by the percent of defective ommatidia, which was quantified through dividing the number of defective (misshapen or merged) ommatidia by the total number of observable ommatidia in each image. All counts were performed manually using the Multi-point Tool on ImageJ (2.3.0, U.S. National Institutes of Health). The number of flies imaged/used for quantification for each experiment is reported in figure captions.

3.4. D-AIP food supplementation

Label-free D-AIP (RGTFEGKF, 940.5 Da) was purchased from BioBasic (Markham, ON, Canada). D-AIP peptides were prepared fresh for each experiment, similar to previously described methods[62]. Briefly, D-AIP peptides were solubilized in batches of 47mg/mL in deionized Milli-Q® water containing 0.1% ammonia. They were vortexed then sonicated at 37hz and 100% power for 10 minutes at 4°C.

All experimental flies were bred and raised in 50mL falcon tubes (Diamed Lab Supplies Inc.) with 5mL of freshly prepared Jazz-Miz *Drosophila* fly food. In treated groups, for a final 5mM concentration of D-AIP, 500µL of freshly solubilized peptides were added to the bottom of the falcon tubes and overlaid with 5mL of newly prepared fly food (cooled to 45°C). The mixture was thoroughly blended and left to solidify overnight. The D-AIP concentration of 5mM is in line with our lab's previous studies and most other studies examining therapeutics in flies[66,67,69].

Genetic crosses of the parental *GMR*-GAL4 driver line and transgenic UAS-Aβ43, UAS-Aβ42, or Canton S lines took place on 5mL of either D-AIP supplemented food or regular food. Parental generation flies were removed from tubes at the appearance of F1 3rd instar larvae. F1 transgenic flies were separated by sex and placed in new D-AIP-supplemented or regular food vials to feed on for 28 days.

3.5. Tissue homogenates

Five flies of each sex, genotype (Aβ43, Aβ42, WT driver line control), and treatment group (for D-AIP experiment) were anesthetized and collected. Flies were snap-frozen in liquid nitrogen then vortexed to separate the heads from bodies, isolating the heads for homogenization (as eye-specific expression of Aβ is of interest). Homogenization of fly heads was performed as previously described[67]. Briefly, fly heads were homogenized in 100µL of PBS-PI (PBS buffer containing Complete EDTA-free Protease Inhibitor Cocktail tablets (Roche))[76], centrifuged for 10 minutes at 12 000g and 4°C, and the supernatant was collected as the 'soluble fraction'. The resulting pellet was resuspended in 50µL of a harsh extraction buffer containing guanidinium hydrochloride (5M GnHCl, 50 mM HEPES pH 7.3, 5 mM EDTA, Complete Protease Inhibitor Cocktail (Roche))[77], then centrifuged again, and the supernatant was then collected as the "insoluble fraction".

3.6. Immunoprecipitation (IP) and Western blot

Aβ43 or Aβ42 were immunoprecipitated from soluble and insoluble homogenate fractions of their respective genotypes using antibody W0-2 (anti-Aβ, epitope residues 4-10; Millipore #MABN10; 5μg of antibody per 25μL of bead slurry) coupled to protein G Sepharose beads (GE Healthcare). Samples were subsequently separated by SDS-PAGE on 10-well 4-12% Bis-Tris gels (NuPAGE), then transferred to 0.45μm nitrocellulose membranes. Membranes were subsequently probed with W0-2 (1: 10 000), followed by anti-mouse horse-radish peroxidase (HRP)-conjugated secondary antibody (Promega # W4021; 1: 10 000) for Aβ43 or Aβ42 detection.

Additionally, for Western blots in the D-AIP food supplementation experiment, corresponding 15μL aliquots of soluble and insoluble fly head homogenate fractions did not undergo immunoprecipitation and were separated by SDS-PAGE on 10-well 4-12% Bis-Tris gels (NuPAGE), then transferred to 0.45μm nitrocellulose membranes. Membranes were probed with an anti-actin antibody (Millipore #MAB1501, 1: 5000), followed by anti-mouse HRP-conjugated secondary antibody (1: 10 000). Western blot data quantification was analyzed using relative ratios of soluble and insoluble Aβ to actin expression levels, to assess any effects of D-AIP on soluble and insoluble Aβ expression levels between treated and non-treated groups.

3.7. Detection and biostability of D-AIP in flies by matrix-assisted laser desorption/ionization time-of-flight (MALDI-TOF) mass spectrometry

For the detection of D-AIP in experimental flies following a 28-day treatment period, flies of each sex, treatment group, and genotype (Aβ43, Aβ42, WT driver line control) were analyzed using MALDI-TOF mass spectrometry, using methods similar to those previously described[67]. Briefly, for each sex, the heads and bodies of 5 flies were isolated, snap-frozen separately using liquid nitrogen, then homogenized in 100μL of PBS-PI (PBS buffer containing Complete EDTA-

free Protease Inhibitor Cocktail tablets (Roche))[76]. 20μL of each homogenate was added to 40μL of methanol, vortexed for 30 seconds, and centrifuged at 13,000rpm for 10 minutes. Supernatants were collected and taken to the McGill SPR-MS Facility, where 1μL of each sample and HCCA matrix (α-Cyano-4-hydroxycinnamic acid) was spotted on the ground steel MALDI-TOF plate using the dried droplet method. A Bruker UltrafleXtreme MALDI-TOF system in reflector positive ionization mode (calibrated mass range of 700 – 5,000 m/z; FlexControl v3.4 software) was used to acquire the spectra**.** Ion intensities were assessed by taking the average of three measurement of 500 shots each (i.e. 2000 shots total per sample).

3.8. Statistical Analyses

Statistical analyses of results obtained from experiments were performed using JASP (0.16.4, JASP Team) and GraphPad Prism (5.0, GraphPad Software Inc.) was used for data presentation. Statistical significance was considered as $p < 0.05$ for all required statistical analyses. Results are presented as mean $\pm$ SEM (Standard Error of Mean). Tests for normality, equality of variances, and outliers were performed on all data. Quantifications of eye toxicity from live confocal imaging micrographs were analyzed using two-way analyses of variance (ANOVA) with sex and treatment group as factors, followed by Tukey's multiple comparison tests. Data with non-normal distributions and/or non equal variances were analyzed using Kruskal-Wallis analyses. Western blot quantifications of relative Aβ levels were analyzed using student t-tests (soluble Aβ fractions, female insoluble Aβ fractions) and one-way t-tests (male insoluble Aβ fractions). No statistical method was used to predetermine sample sizes and no blinding was performed.

4. RESULTS

4.1. Confirmation of human Aβ43 expression in transgenic *Drosophila melanogaster*

UAS-Aβ43 transgenic *Drosophila melanogaster* were received from the lab of Linda Partridge[47]. Following PCR experiments which successfully confirmed the presence of the human Aβ43 transgene in these flies, a genetic cross between UAS-Aβ43 flies and *GMR*-GALl4 flies was performed on regular fly food to produce transgenic Aβ43-expressing progeny. Expression of Aβ43 in the heads of both male and female progeny was confirmed via Western Blotting of immunoprecipitated Aβ from homogenates using the anti-Aβ antibody W0-2 **(Figure 2).** Bands were visible at the expected molecular weight of Aβ43 (approximately 4.6kDa) in the Western blots of both soluble and insoluble fractions**.** As controls for positive and negative Aβ expression, immunoprecipitated Aβ from homogenates of Aβ42-expressing or *GMR*-GAL4 driver control fly heads were run alongside Aβ43 fly samples. Bands were visible at the expected molecular weight of Aβ42 (approximately 4.5kDa), while no bands were detected in the lanes of *GMR*-GAL4 driver control fly homogenates **(Figure 2).**

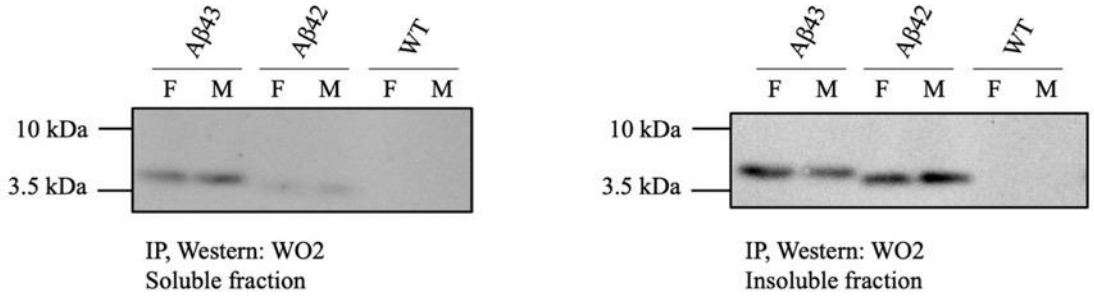

Figure 2. Aβ43 is expressed in the heads of transgenic *Drosophila melanogaster*
Western blots of Aβ immunoprecipitated from fly head extracts of eye (*GMR*-driven) expression of Aβ43, Aβ42, or no transgene (WT), using the anti-Aβ W0-2 antibody. Western blots from immunoprecipitation experiments performed on the 'soluble' and 'insoluble' fractions of fly head homogenates are displayed on the left and right, respectively. Flies were aged for 36 days. Five fly heads per sex and genotype were used.

4.2. Eye-directed expression of human Aβ43 in *Drosophila melanogaster* results in a longitudinal toxic "rough eye" phenotype

Upon the confirmation of induced Aβ43 expression in these transgenic flies, live confocal imaging was performed to investigate eye toxicity induced by the eye-directed expression of Aβ43. Morphology of the compound eye was longitudinally evaluated, and the levels of induced toxicity ("rough eye" phenotype) were quantified using the ratio of misshapen ommatidia: total ommatidia. Eye morphology was evaluated through assessing ommatidial shape and organization of the compound eye, as outlined in **Figure 3**. Transgenic flies with eye-directed expression of Aβ42 (known model of eye toxicity induced by Aβ42) and *GMR*-GAL4 driver control flies were also evaluated. The penetrance of the rough eye phenotype was 100% in both Aβ43- and Aβ42-expressing transgenic flies at both time points.

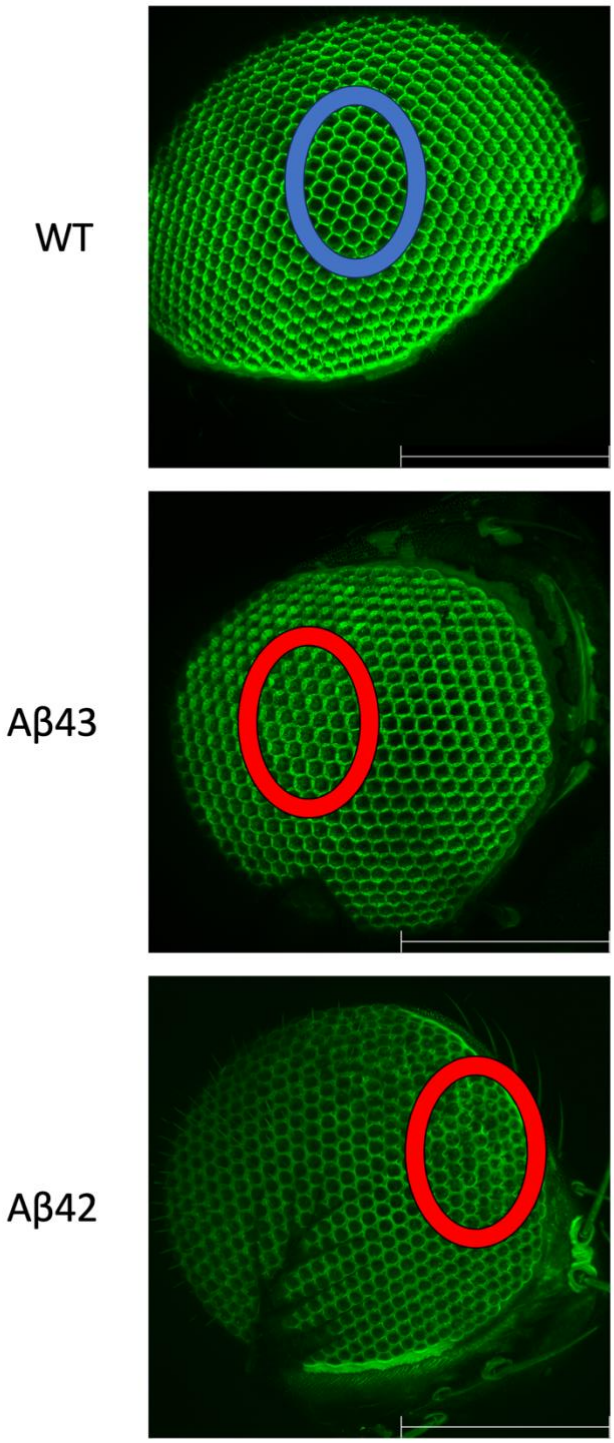

Figure 3. Evaluation of ommatidial shape and organization in *Drosophila melanogaster* compound eye

Representative images of 28-day post-eclosion female *Drosophila* compound eyes captured using live confocal imaging, demonstrating differences in ommatidial shape and organization evaluated for the quantification of Aβ-induced eye toxicity. While wildtype (WT, top panel) flies possess hexagonal ommatidia and symmetrical ommatidial organization (circled in blue), transgenic flies expressing either Aβ43 (middle panel) or Aβ42 (bottom panel) display non-hexagonal, fused, or square shaped ommatidia, and/or non-symmetrical ommatidial organization (circled in red). Scale bar: 200μm.

Live confocal imaging was performed at five days post-eclosion and 28 days post-eclosion. At five days post-eclosion, Aβ43-expressing flies demonstrated morphological abnormalities of ommatidial shape (i.e., square or non-hexagonal lens facets) and organization in both male and female flies **(Figure 4A)**. Severe deformations of ommatidia structure were observed in eye specific Aβ42 transgenic flies of both sexes, with fused lens facets, misshapen ommatidia, and general ommatidial disorganization of the compound eye **(Figure 4A)**. No substantial morphological changes in the shape of organization of ommatidia were observed in *GMR*-GAL4 driver control flies, regardless of sex (**Figure 4A)**. Two-way ANOVA analyses were performed on micrograph quantifications of eye toxicity for each of the two time points, with sex and genotype as factors. At five days post-eclosion, there was a significant effect of genotype on the percent of eye toxicity, $F(2, 13) = 51.972$, $p < 0.001$ **(Figure 4B)**. Post-hoc analyses using Tukey's pairwise comparisons correction demonstrated significant differences in eye toxicity between all three genotypes: Aβ43 transgenic flies (mean = 40.8 ± 6.2%) and Aβ42 transgenic flies (mean = 86.6 ± 3.3%) both demonstrated significantly increased eye toxicity quantifications than *GMR*-GAL4 driver control flies (mean = 18.4 ± 3.3%), $p = 0.015$ and $p < 0.001$, respectively. Aβ43 transgenic flies exhibited significantly lower eye toxicity quantifications than Aβ42 transgenic flies, $p < 0.001$. No significant interaction effect was found between genotype and sex, $F(2, 13) = 0.131$, $p = 0.879$, and no significant effect of sex on eye toxicity quantifications was found, $F(1, 13) = 0.035$, $p = 0.854$.

The same cohort of flies was aged 28 days, then individually imaged using live confocal microscopy to examine eye morphology and induced toxicity at a later stage of life (**Figure 5A)**. Male and female Aβ43 transgenic flies demonstrated more pronounced morphological abnormalities in ommatidial shape and general organization, while Aβ42 transgenic flies of both

sexes had sustained its morphology from five days post-eclosion, with severe deformations of ommatidial shape, organization, and structure of the compound eye. Consistent with observations at five days post-eclosion, no substantial morphological changes in the shape of organization of ommatidia were observed in *GMR*-GAL4 driver control flies of either sex. A two-way ANOVA analysis performed on eye toxicity quantifications revealed a significant effect of genotype of on eye toxicity, $F(2, 19) = 251.351$, $p < 0.001$ (**Figure 5B)**. Post-hoc analyses using Tukey's pairwise comparisons correction demonstrated again that both Aβ43 (mean = 53.5 ± 2.0%) and Aβ42 transgenic flies (mean = 89.2 ± 1.3%) had significantly higher quantifications of eye toxicity than *GMR*-GAL4 driver control flies (mean = 17.9 ± 2.5%), $p < 0.001$ for both comparisons. Aβ43 transgenic flies maintained a significantly lower quantification of eye toxicity, $p < 0.001$. No significant interaction effect was found between genotype and sex, $F(2, 19) = 1.602$, $p = 0.228$, and no significant effect of sex on eye toxicity quantifications was found, $F(1, 19) = 1.050$, $p = 0.318$.

A

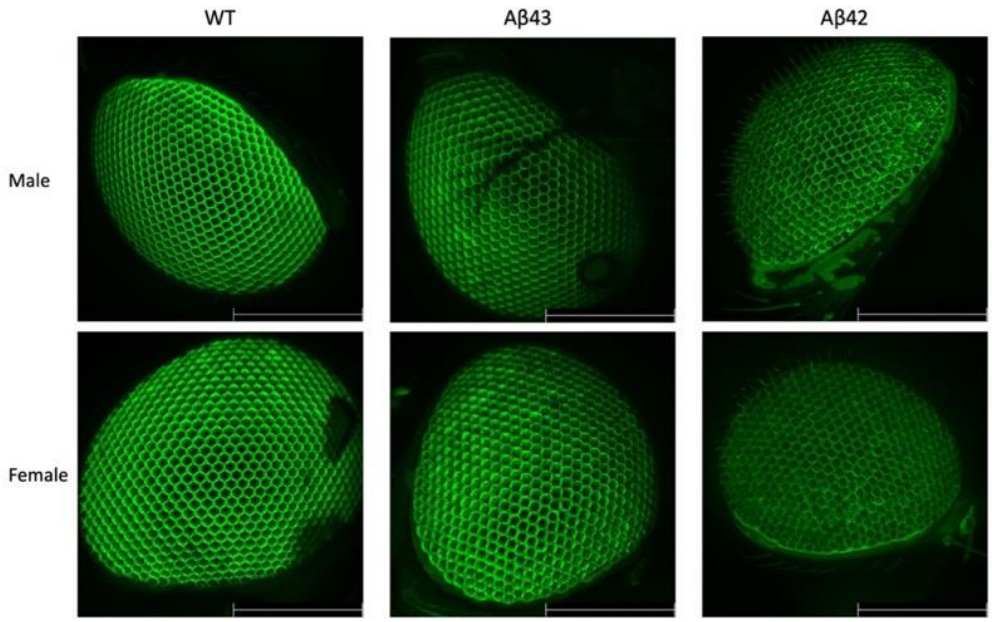

B

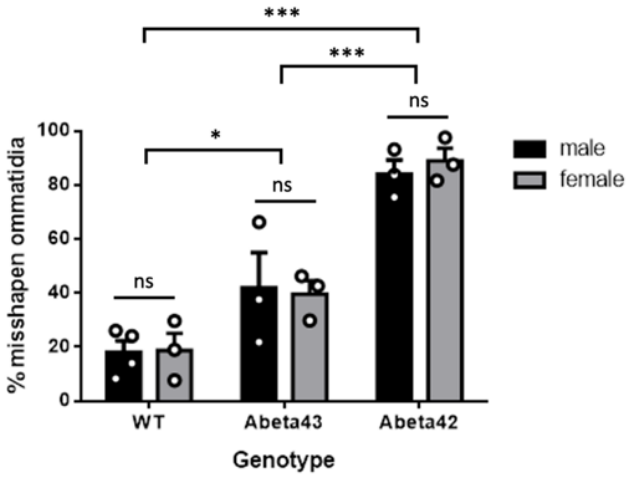

Figure 4. Expression of human Aβ43 in the eyes of *Drosophila melanogaster* results in a "rough eye" phenotype at day five post-eclosion

A. Representative live confocal images of transgenic male and female *Drosophila* compound eyes at five days post eclosion for driver line control (WT) flies (mildly disrupted morphology), Aβ43 transgenic flies (disrupted morphology), and Aβ42 transgenic flies (disrupted morphology). Scale bar: 200μm. **B.** Quantification of the percent of misshapen ommatidia in male and female WT, Aβ43, and Aβ42 transgenic flies at five days post-eclosion. Data is represented as mean ± SEM. Statistical analyses were performed using a two-way ANOVA followed by Tukey's pairwise comparison tests. No significant effect of sex on eye toxicity and no interaction effect was found. The percent of misshapen ommatidia significantly differed between each genotype: $*p = 0.015$, WT vs. Aβ43; $***p < 0.001$, Aβ43 vs. Aβ42; $***p < 0.001$, WT vs. Aβ42. Three to four flies were imaged per sex for each genotype.

A

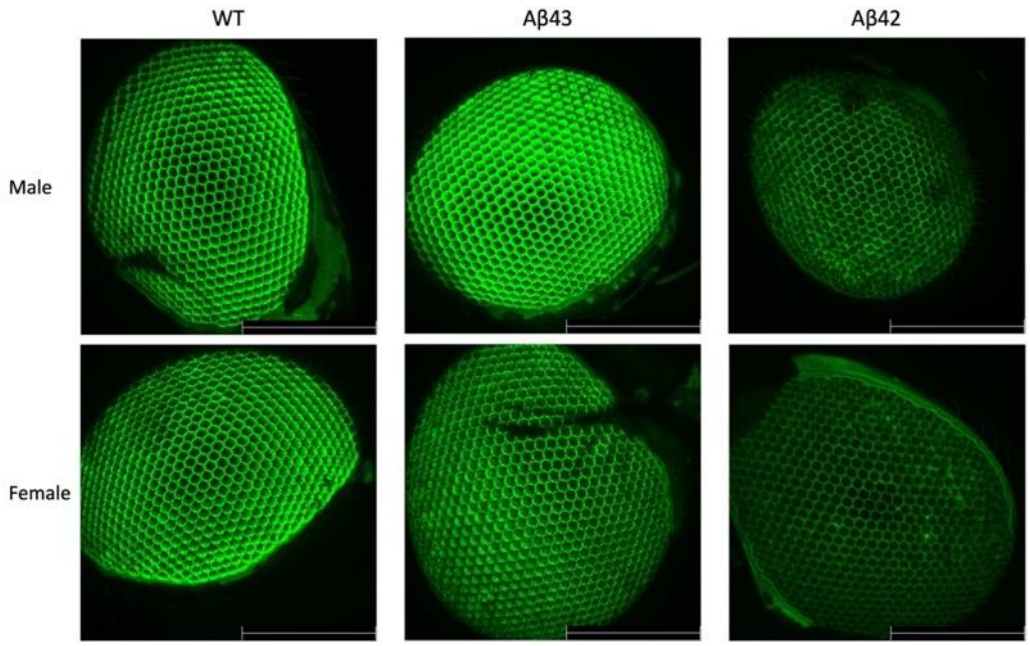

B

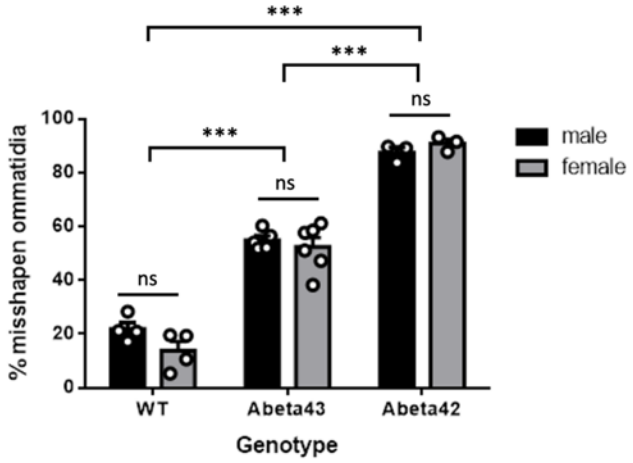

Figure 5. Expression of human Aβ43 in the eyes of *Drosophila melanogaster* results in a "rough eye" phenotype at day 28 post-eclosion

A. Representative live confocal images of transgenic male and female *Drosophila* compound eyes at 28 days post-eclosion for driver line control (WT) flies (mildly disrupted morphology), Aβ43 transgenic flies (disrupted morphology), and Aβ42 transgenic flies (disrupted morphology). Scale bar: 200μm. **B**. Quantification of the percent of misshapen ommatidia in male and female WT, Aβ43, and Aβ42 transgenic flies at 28 days post-eclosion. Data is represented as mean ± SEM. Statistical analyses were performed using a two-way ANOVA followed by Tukey's pairwise comparison tests. No significant effect of sex on eye toxicity and no interaction effect was found. The percent of misshapen ommatidia significantly differed between each genotype: ****p* <0.001, WT vs. Aβ43; ****p* <0.001, Aβ43 vs. Aβ42; ****p* <0.001, WT vs. Aβ42. Three to six flies were imaged per sex for each genotype.

4.3. Detection of D-AIP in the heads and bodies of transgenic *Drosophila melanogaster* at 28 days post-eclosion

MALDI-TOF mass spectrometry was performed by Dr. Mark Hancock to confirm the uptake of D-AIP in transgenic *Drosophila melanogaster*. *Drosophila* with eye-specific expression of either Aβ43, Aβ42, or *GMR*-GAL4 control flies were bred and raised for 28 days on either D-AIP supplemented or non-supplemented food, then snap-frozen for MALDI-TOF analyses. Prior to analyzing *Drosophila* homogenates, calibration of a peptide standard **(Figure 6A)** was performed, followed by label-free detection of D-AIP (940.477 Da + 1H+ = 941.477 *m/z*) from serial dilutions of a 5mM D-AIP stock **(Figure 6B)**. The 941.477 *m/z* peak was present in the spectra from homogenates of isolated heads **(Figure 7A)** and bodies **(Figure 7B)** of female flies in D-AIP treated groups across all genotypes. Likewise, the 941.477 *m/z* peak was also present in the spectra from homogenates of isolated heads **(Figure 8A)** and bodies **(Figure 8B)** of male flies in D-AIP treated groups across all genotypes. In contrast, across all genotypes, the 941.477 *m/z* peak was not present in any spectra from homogenates of fly heads or bodies in the non-treated groups of either sex **(Figure 7-8)**.

A

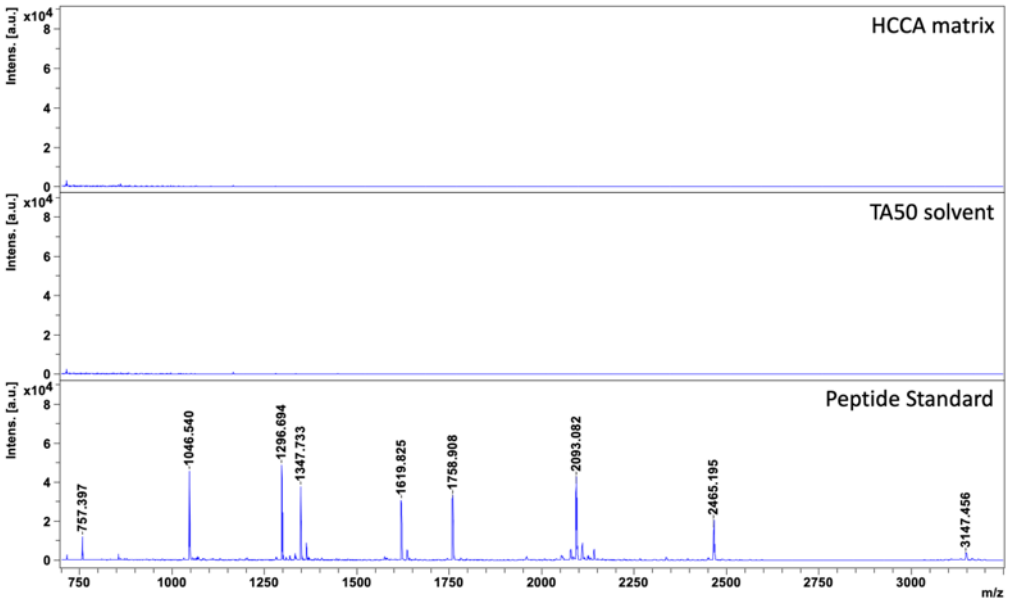

B

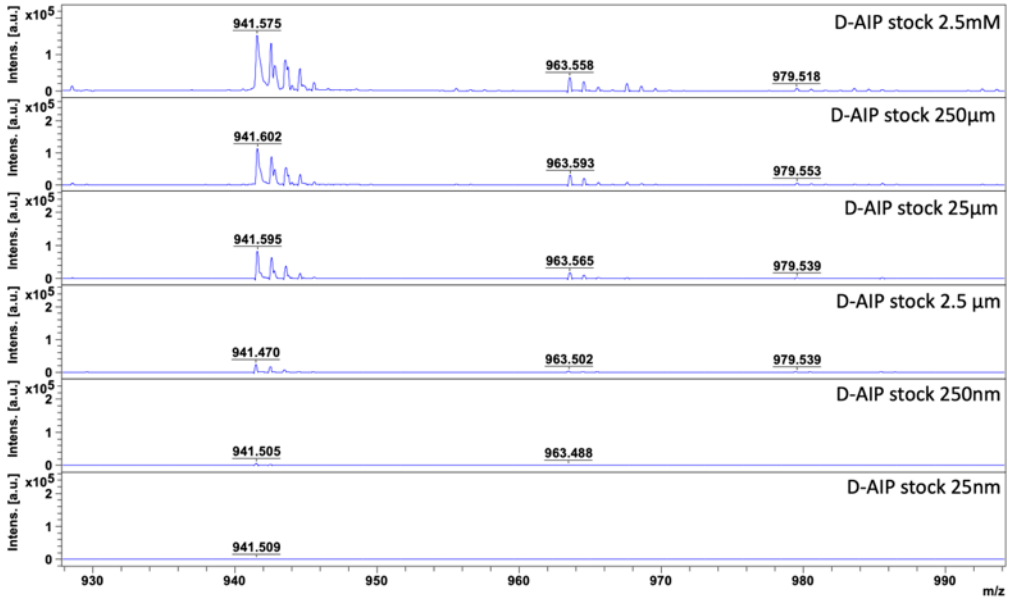

Figure 6. Calibration of MALDI mass spectrometer and standard D-AIP dilution series
A. Representative spectra for HCCA matrix alone (top), TA50 solvent alone (middle), and Bruker peptide calibration standard spotted 1:1 with HCCA matrix solution (bottom). **B.** Representative spectra for the label-free detection of D-AIP standard (5mM in 0.1% ammonia water) serially diluted in TA50 solution. Both the sodium (940.477 Da + 23 Na+ = 963.477 *m/z*) and potassium (940.477 Da + 39 K+ = 979.477 *m/z*) adducts were detected in addition to the isotopic distribution for D-AIP (940.477 Da + 1 H+ = 941.477 *m/z*).

A

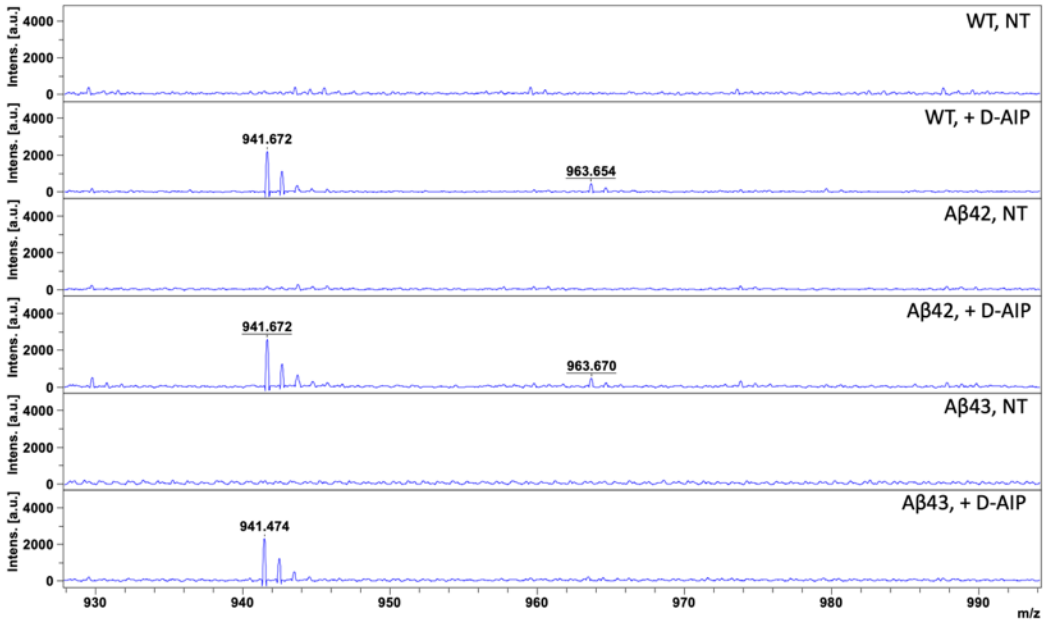

B

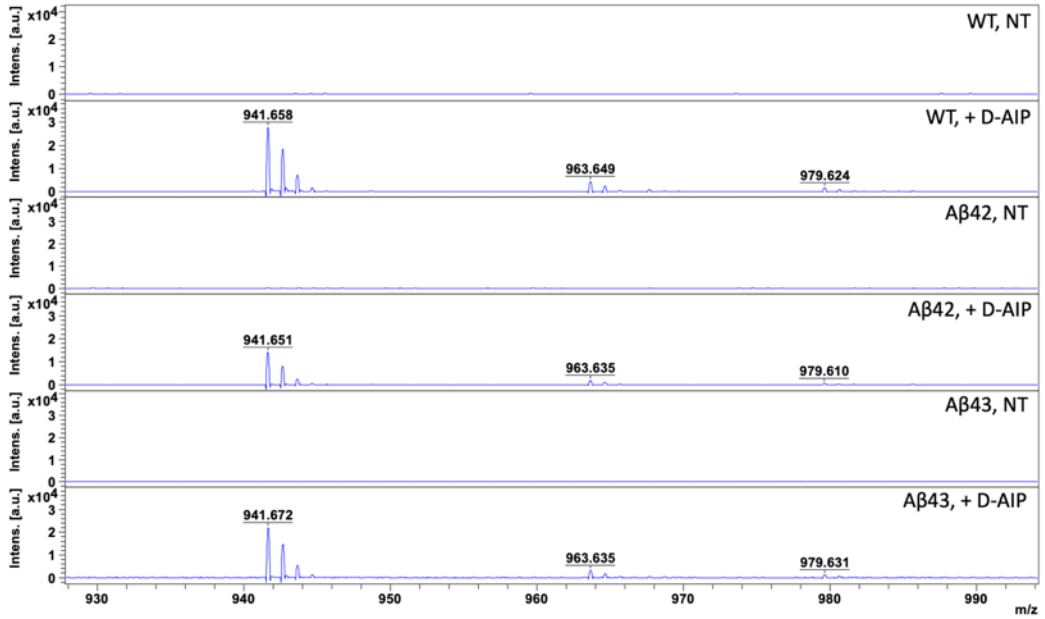

Figure 7. Detection of D-AIP in homogenates of transgenic female *Drosophila melanogaster* by MALDI-TOF mass spectrometry.

A. Representative spectra for the label-free detection of D-AIP (941.477 *m/z* and/or Na+ / K+ adducts) in the heads and **B.** bodies of female transgenic *GMR*-GAL4 control (WT), Aβ42-expressing, and Aβ43-expressing flies that were bred and raised for 28 days on D-AIP supplemented food. Five flies were used per genotype and treatment condition.

A

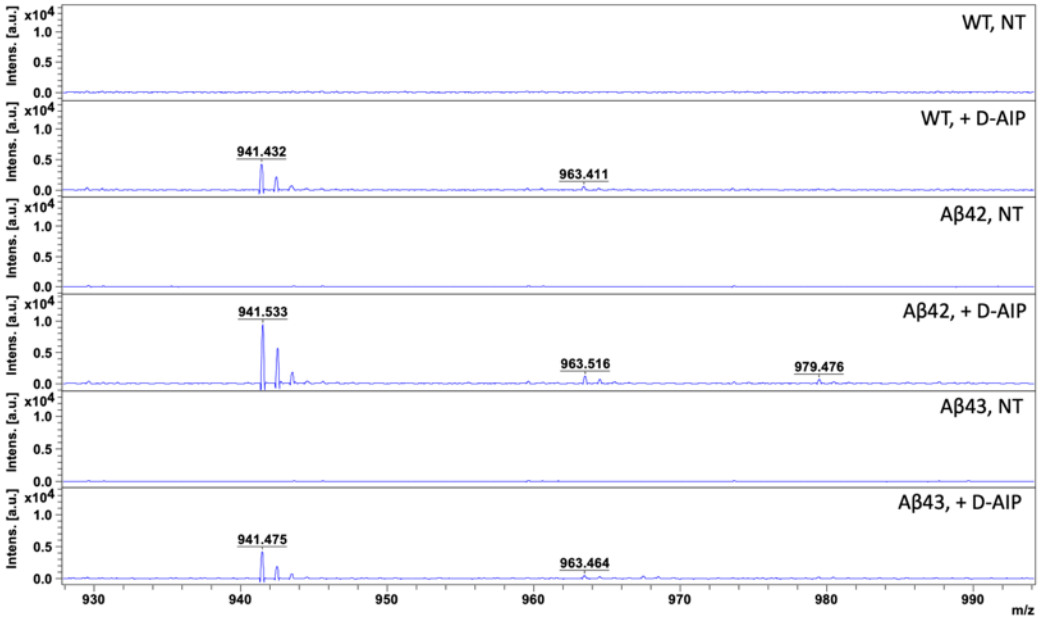

B

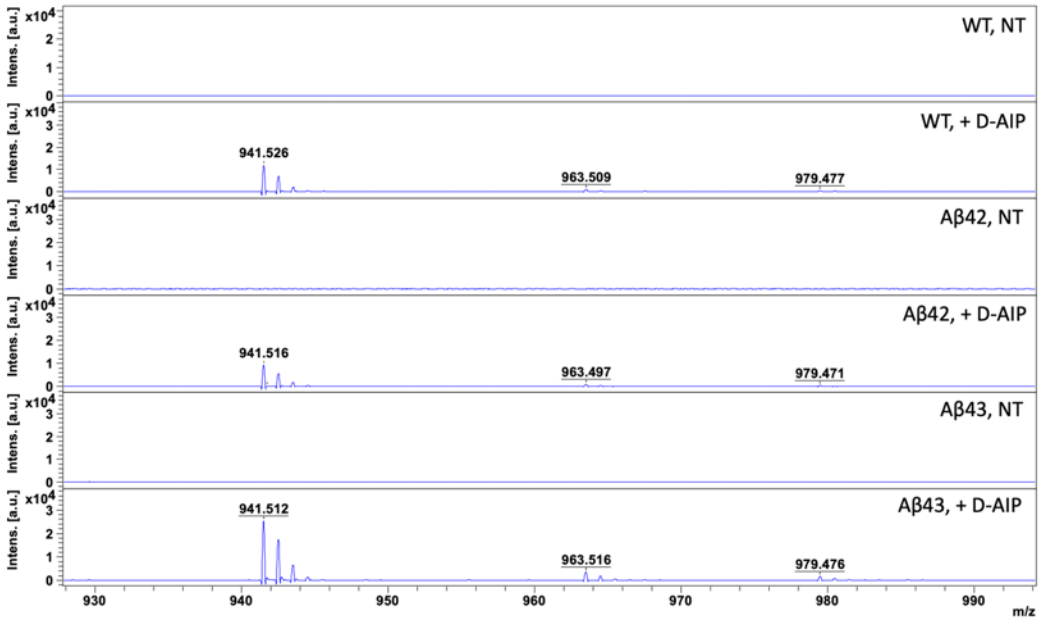

Figure 8. Detection of D-AIP in homogenates of transgenic male *Drosophila melanogaster* by MALDI-TOF mass spectrometry.

A. Representative spectra for the label-free detection of D-AIP (941.477 *m/z* and/or Na+ / K+ adducts) in the heads and **B.** bodies of male transgenic *GMR*-GAL4 control (WT), Aβ42-expressing, and Aβ43-expressing flies that were bred and raised for 28 days on D-AIP supplemented food. Five flies were used per genotype and treatment condition.

4.4. D-AIP consumption does not significantly affect levels of Aβ43 in the heads transgenic *Drosophila melanogaster* after 28 days of treatment

Transgenic flies with eye-directed expression of Aβ43 were bred and raised for 28 days on either D-AIP supplemented or non-supplemented food, snap-frozen, and their heads were subsequently isolated for analysis of Aβ43 levels. Western blots were performed on immunoprecipitated samples of soluble Aβ43 fractions (monomers, oligomers, protofibrils) and insoluble Aβ43 fractions (fibrils) **(Figure 9A)**. Quantification of relative Aβ43 levels in D-AIP treated and non-treated groups were performed using corresponding actin levels for both soluble and insoluble Aβ43 fractions **(Figure 9B)**. Student's t-tests demonstrated no significant differences in mean levels of soluble Aβ43 between D-AIP treated and non-treated female flies, $t(6) = 0.691$, $p = 0.516$, and male flies, $t(6) = 0.142$, $p = 0.892$. A student t-test and one-way t-test also demonstrated no significant difference in mean levels of insoluble Aβ43 between D-AIP treated and non-treated female flies, ($t(6) = -2.254$, $p = 0.065$) and male flies ($t(3) = -0.837$, $p = 0.464$) respectively.

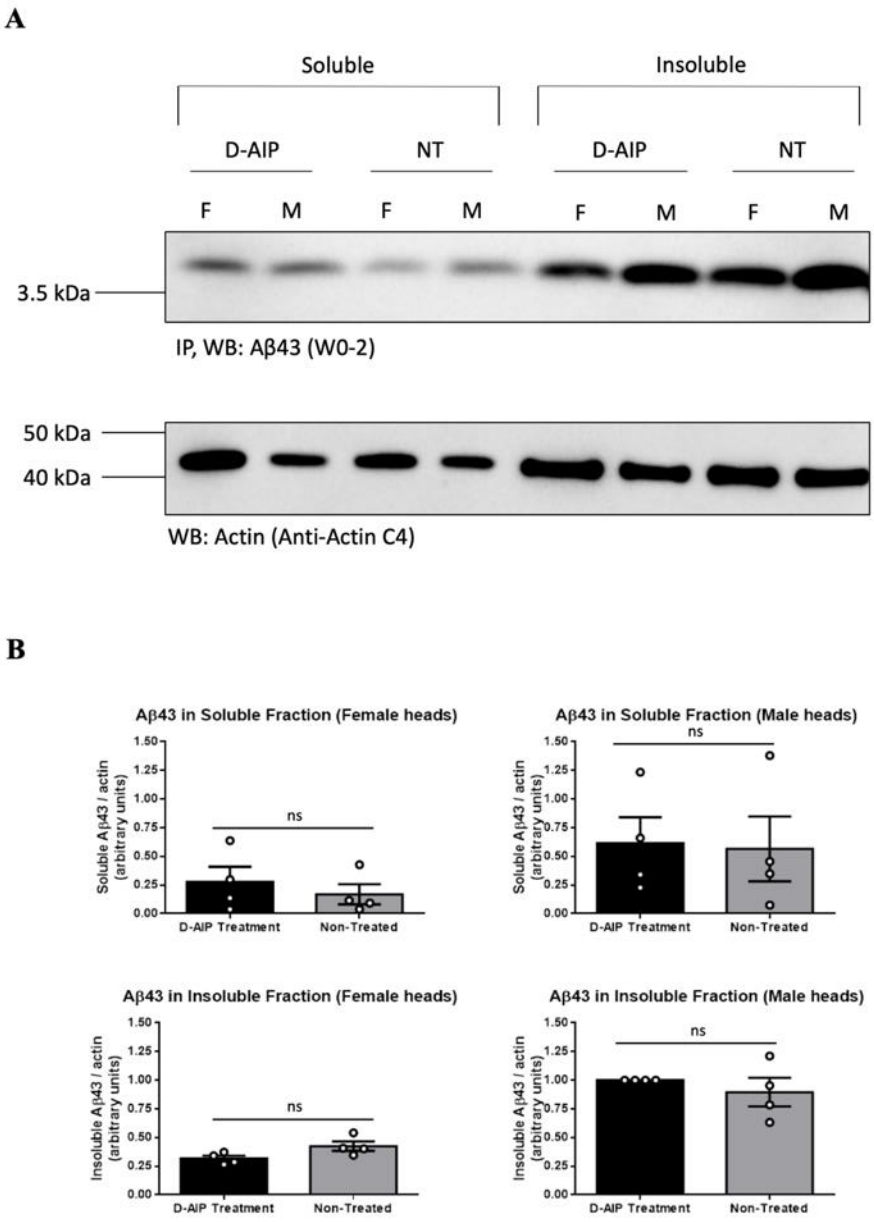

Figure 9. Levels of Aβ43 in transgenic *Drosophila melanogaster* are not significantly affected after a 28-day treatment period of D-AIP food supplementation

A. Representative Western blots of soluble and insoluble Aβ43 fractions, immunoprecipitated from fly head extracts of transgenic *Drosophila melanogaster* with eye-driven expression of Aβ43. Flies were bred and raised for 28 days on either regular or D-AIP supplemented food. Five fly heads were used for each sex per treatment condition. **B.** Quantification of relative Aβ43 levels from Western blot data. T-tests demonstrated no significant differences in soluble or insoluble Aβ43 levels in flies of either sex in the D-AIP treated group compared to the non-treated group: $p = 0.516$ (Student's t-test, female soluble fraction), $p = 0.892$ (Student's t-test, male soluble fraction), $p = 0.065$ (Student's t-test, female insoluble fraction), $p = 0.464$ (One-way t-test, male insoluble fraction). Data is represented as mean ± SEM, n = 4.

4.5. D-AIP consumption does not significantly affect levels of Aβ42 in the heads transgenic *Drosophila melanogaster* after 28 days of treatment

Analogous to transgenic Aβ43-expressing flies, transgenic flies with eye-directed expression of Aβ42 were bred and raised for 28 days on either D-AIP supplemented or non-supplemented food. For analysis of Aβ42 levels in the head, flies from both treatment groups were snap-frozen and their heads were isolated. Western blots were then performed on immunoprecipitated samples of soluble (monomers, oligomers, protofibrils) and insoluble Aβ42 fractions (fibrils) **(Figure 10A)**. Quantification of relative Aβ42 levels in D-AIP treated and non-treated groups were performed using corresponding actin levels for both soluble and insoluble Aβ42 fractions **(Figure 10B)**. Student's t-tests resulted in no significant difference in mean soluble Aβ42 levels in the D-AIP treated group compared to the non-treated group, in both females ($t(6) = 0.207$, $p = 0.843$) and males ($t(6) = -0.744$, $p = 0.485$). Further, Student's t-test resulted in no significant difference of mean insoluble Aβ42 levels in the D-AIP treated group compared to the non-treated group in female flies, ($t(5) = 0.396$, $p = 0.708$), and a One-sample t-test also resulted in no significant difference of mean insoluble Aβ42 levels in the D-AIP treated group compared to the non-treated group in male flies, ($t(3) = 1,574$, $p = 0.214$).

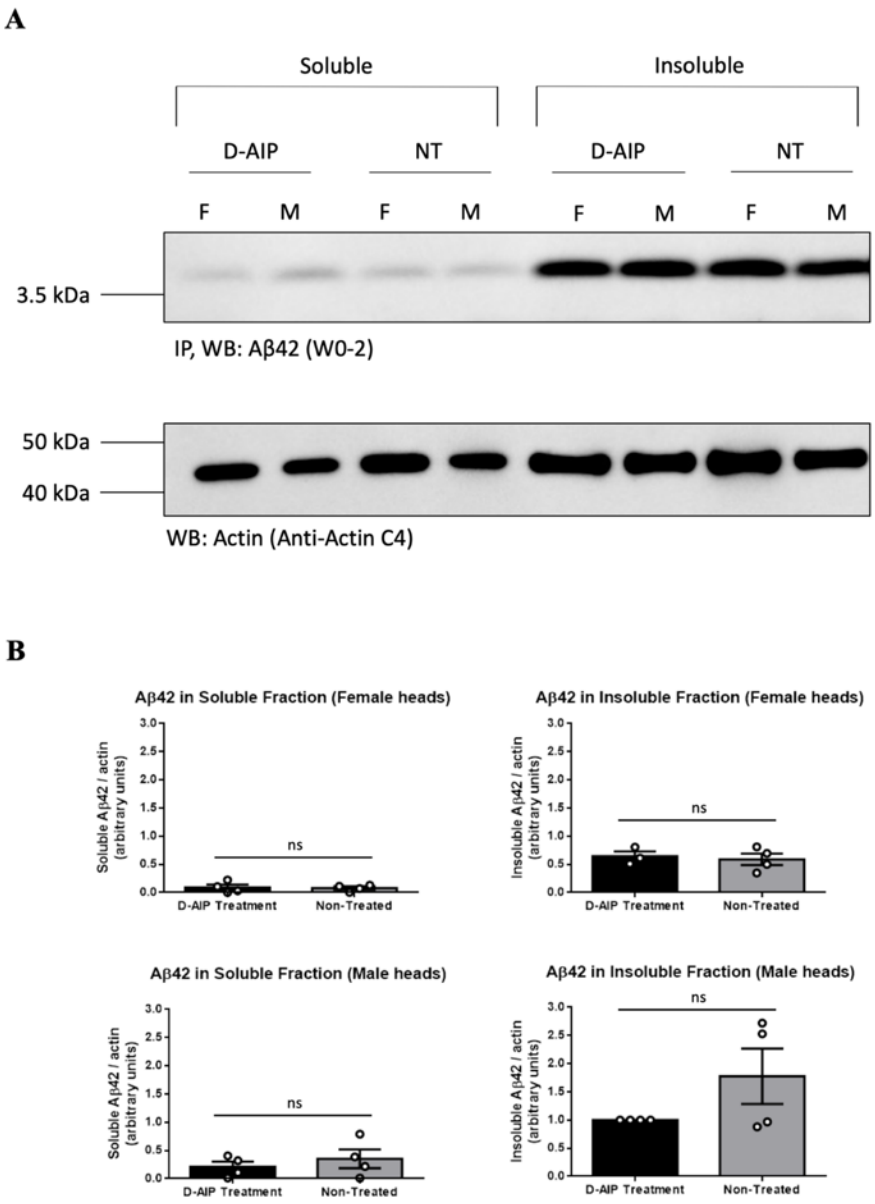

Figure 10. Levels of Aβ42 in transgenic *Drosophila melanogaster* are not significantly different after a 28-day treatment period of D-AIP food supplementation

A. Representative Western blots of soluble and insoluble Aβ42 fractions, immunoprecipitated from fly head extracts of transgenic *Drosophila melanogaster* with eye-driven expression of Aβ42. Flies were bred and raised for 28 days on either regular or D-AIP supplemented food. Five fly heads were used for each sex per treatment condition. **B.** Quantification of relative Aβ42 levels from Western blot data. One data point (from female, D-AIP treated, insoluble fraction) was an outlier and therefore excluded from analyses. T-tests demonstrated no significant differences in soluble or insoluble Aβ42 levels in flies of either sex in the D-AIP treated group compared to the non-treated group: $p = 0.843$ (Student's t-test, female soluble fraction), $p = 0.485$ (Student's t-test, male soluble fraction), $p = 0.708$ (Student's t-test, female insoluble fraction). $p = 0.214$ (One-way t-test, male insoluble fraction). Data is represented as mean ± SEM, n = 4.

4.6. D-AIP does not affect longevity of transgenic *Drosophila melanogaster*

Kaplan-Meier survival curve analyses were used to assess the longevity of transgenic *Drosophila melanogaster* with eye-specific expression of either Aβ43, Aβ42, or *GMR*-GAL4 control flies **(Figure 11)**. Transgenic flies were bred and raised on either D-AIP supplemented or non-supplemented food, separated by sex, and their survival counts were recorded for a 28-day treatment period. To determine if D-AIP treatment affected longevity of transgenic *Drosophila melanogaster*, log-rank tests were used to compare Kaplan-Meier survival curves of transgenic flies feeding on D-AIP supplemented or non-supplemented food. No significant differences in longevity were found between D-AIP treated and non-treated groups in either sex of Aβ43 flies (female: $\chi^2(1) = 1.377$, $p = 0.241$; male: $\chi^2(1) < 0.001$, $p = 0.991$), Aβ42 flies (female: $\chi^2(1) < 0.001$, $p = 0.979$; male: $\chi^2(1) = 0.678$, $p = 0.411$), or *GMR*-GAL4 control flies (female: $\chi^2(1) = 0.678$, $p = 0.411$; male: $\chi^2(1) = 1.000$, $p = 0.317$).

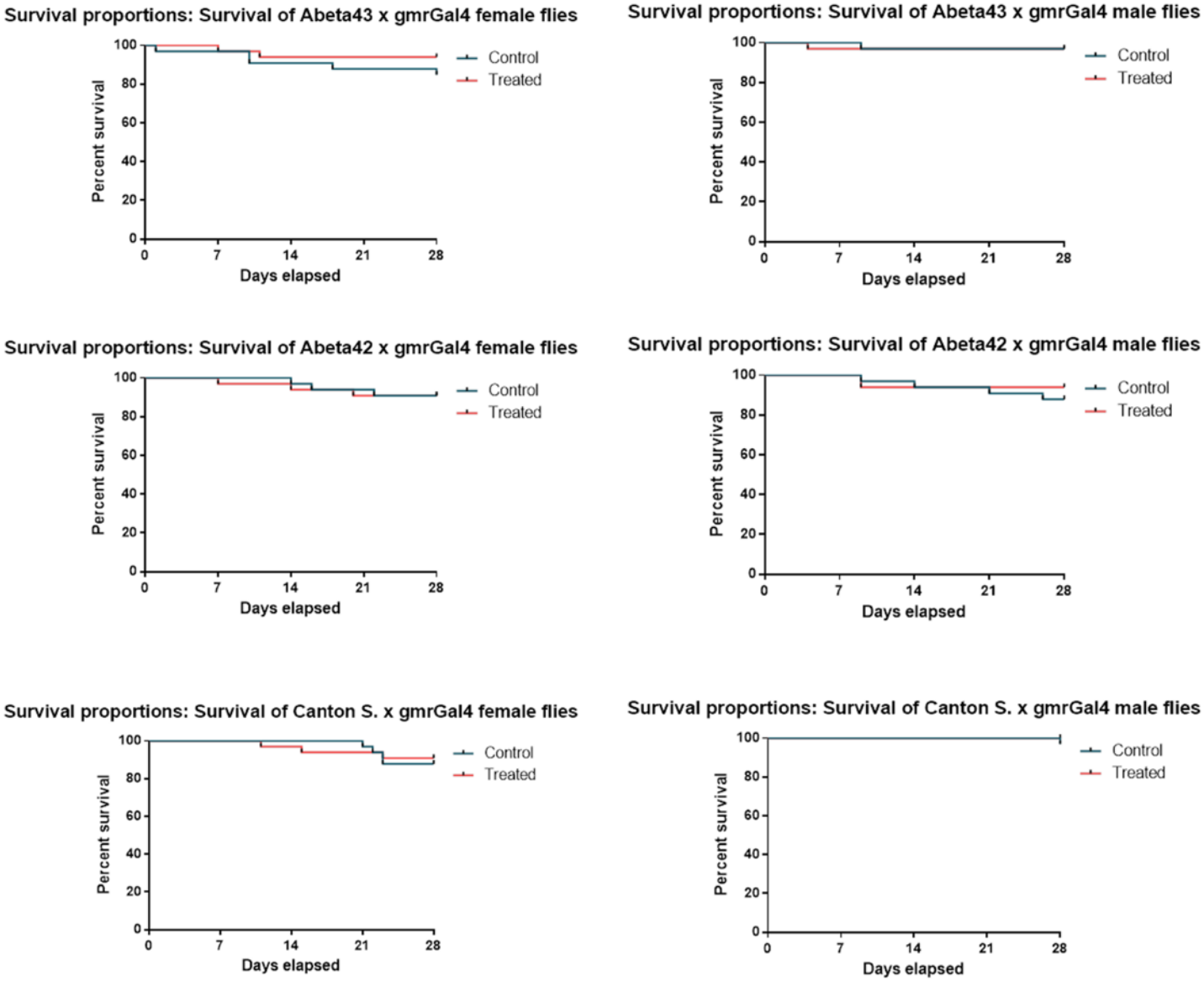

Figure 11. Kaplan-Meier survival curves of transgenic *Drosophila melanogaster* for a 28-day treatment period of D-AIP food supplementation

Survival curves of transgenic flies with eye-directed expression of Aβ43, Aβ42, or driver line control flies, bred and raised for 28 days on either regular or D-AIP supplemented food. Log-rank analyses demonstrate that D-AIP treatment has no significant effect on longevity Aβ43-expressing, Aβ42-expressing, or driver line control flies of either sex ($p > 0.05$ for all comparisons), 11 flies per group, n = 3.

4.7. D-AIP attenuates the Aβ43-induced toxic "rough eye" phenotype in transgenic *Drosophila melanogaster* at five, 14, and 28 days post-eclosion

Transgenic *Drosophila melanogaster* with eye-directed expression of Aβ43 were bred and raised for 28 days on either D-AIP supplemented or non-supplemented food. Using live confocal microscopy, flies were individually imaged at five, 14, and 28 days post-eclosion to assess and quantify their compound eye morphology **(Figures 12-14)**. Two-way ANOVA analyses were performed on micrograph quantification data of percent of misshapen ommatidia for five and 14 days post-eclosion, while non-parametric Kruskal-Wallis tests were performed on 28 days post-eclosion micrograph quantification data, due to unequal variances between groups. D-AIP demonstrated a significant effect on the percent of misshapen ommatidia (toxic "rough eye" phenotype) at five days post eclosion, $F(1, 34) = 5.863$, $p = 0.021$, 14 days post-eclosion, $F(1, 12) = 16.972$, $p = 0.001$, and 28 days post-eclosion, $H(1) = 24.674$, $p < 0.001$; transgenic flies in the D-AIP-treated group exhibited a significantly lower (day five: mean (female) = 59.30%, mean (male) = 47.47%; day 14: mean (female) = 67.04%, mean (male) = 49.32%; day 28: median (female) = 67.35%, median (male) = 61.22%) percentage of misshapen ommatidia compared to the non-treated group (day five: mean (female) = 74.61%, mean (male) = 68.43%; day 14: mean (female) = 82.45%, mean (male) = 76.52%; day 28: median (female) = 90.69%, median (male) = 91.36%). There was no significant effect of sex on "rough eye" phenotype at five days post-eclosion, $F(1, 34) = 1.447$, $p = 0.237$ and 28 days post-eclosion, $H(1) = 0.151$, $p = 0.697$. However, sex had a significant effect on "rough eye" phenotype at 14 days post-eclosion, $F(1, 12) = 5.231$, $p = 0.041$. Further, no significant interaction between sex and treatment group was found at day five, $F(1, 34) = 0.142$, $p = 0.708$ or day 14, $F(1, 12) = 1.299$, $p = 0.277$.

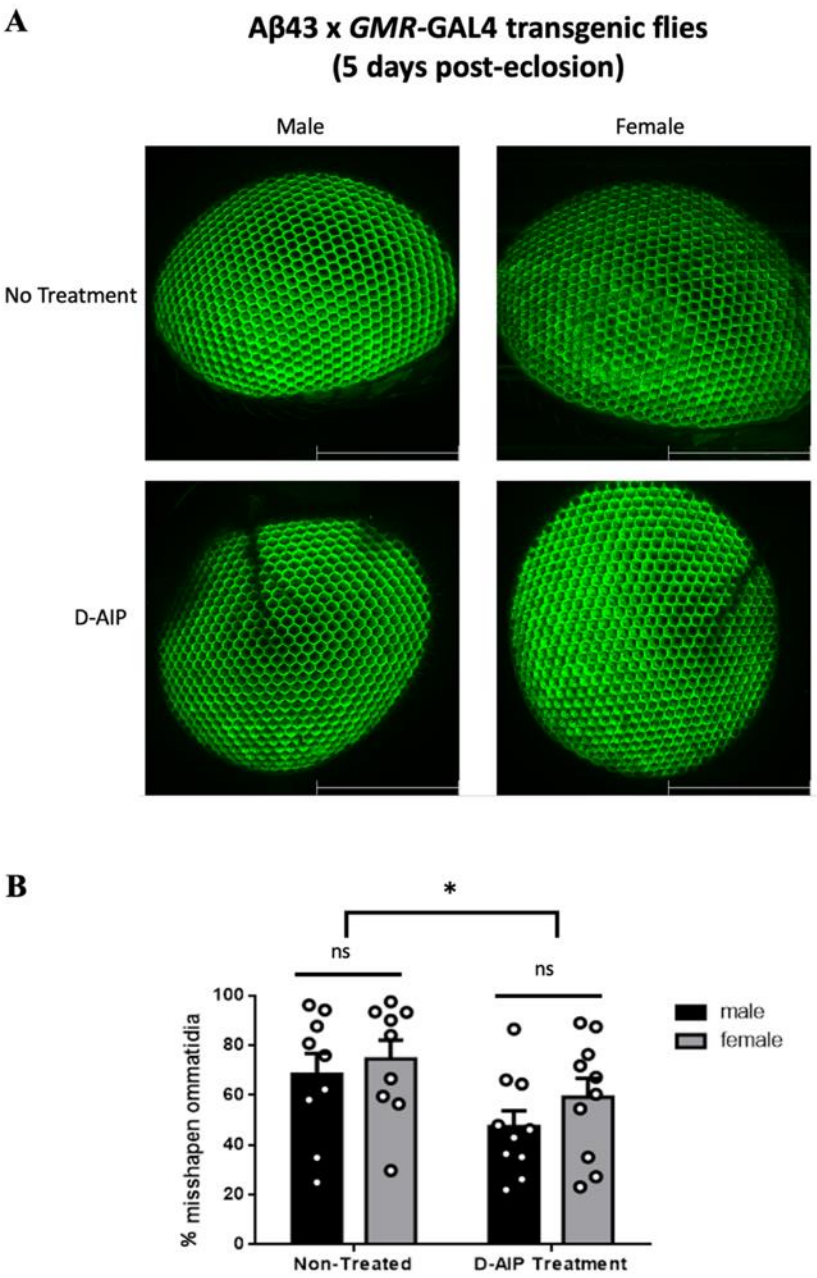

Figure 12. D-AIP treatment attenuates Aβ43-induced eye toxicity in transgenic flies at five days post-eclosion

A. Representative live confocal images of transgenic Aβ43-expressing *Drosophila melanogaster* compound eyes at five days post-eclosion, feeding on either regular or D-AIP supplemented food. Scale bar: 200μm. **B.** Quantification of percent of misshapen ommatidia. A two-way ANOVA analysis was performed, revealing that D-AIP treatment significantly reduced the percent of misshapen ommatidia, $*p = 0.021$. No significant effect of sex on eye toxicity and no interaction effect between sex and treatment was found, $p > 0.05$. Data is represented as mean ± SEM. Two to three flies were imaged per treatment replicate, n = 4.

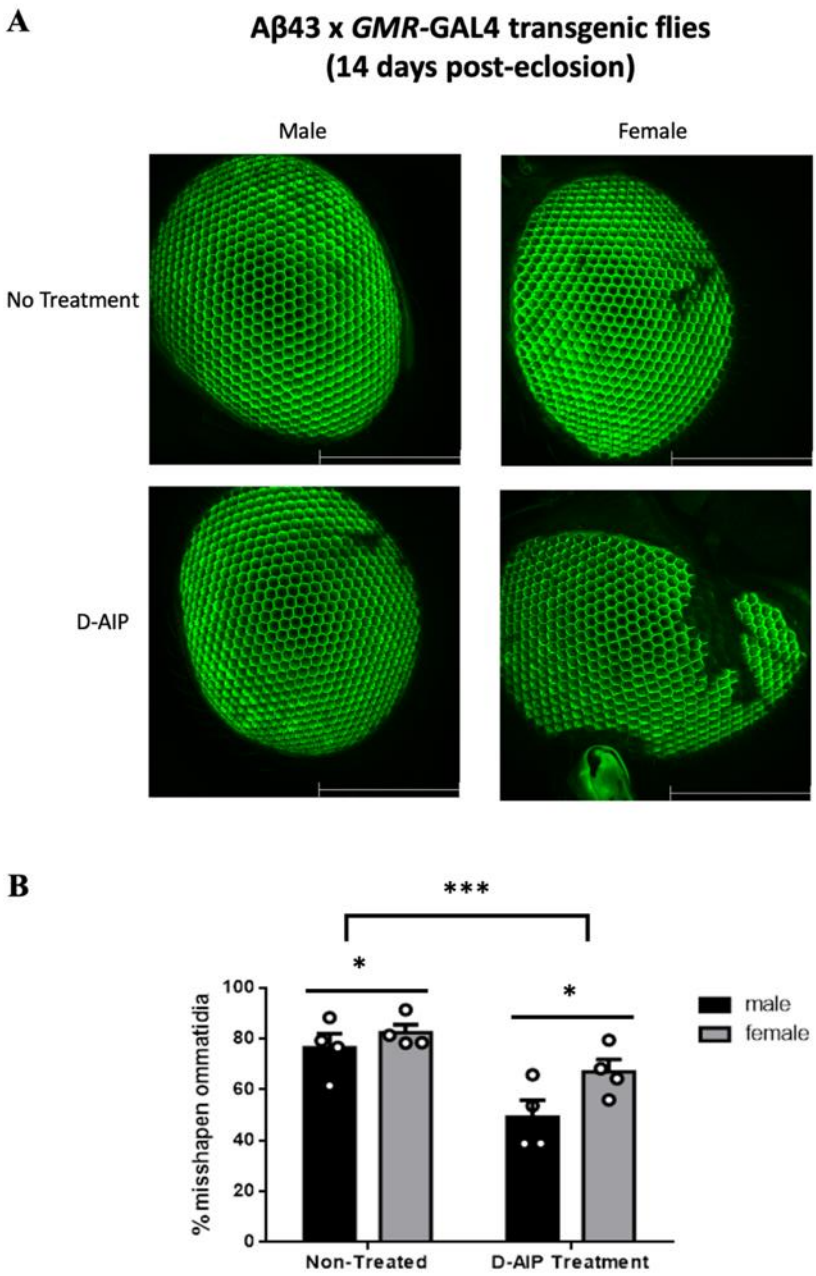

Figure 13. D-AIP treatment attenuates Aβ43-induced eye toxicity in transgenic flies at 14 days post-eclosion

A. Representative live confocal images of transgenic Aβ43-expressing *Drosophila melanogaster* compound eyes at 14 days post-eclosion, feeding on either regular or D-AIP supplemented food. Scale bar: 200μm. **B.** Quantification of percent of misshapen ommatidia. A two-way ANOVA analysis was performed, revealing that D-AIP treatment significantly reduced the percent of misshapen ommatidia, ***$p = 0.001$. There was a significant effect of sex on percent of misshapen ommatidia, *$p = 0.041$. No interaction effect between sex and treatment was found, $p > 0.05$. Data is represented as mean ± SEM. One fly was imaged per treatment replicate, n = 4.

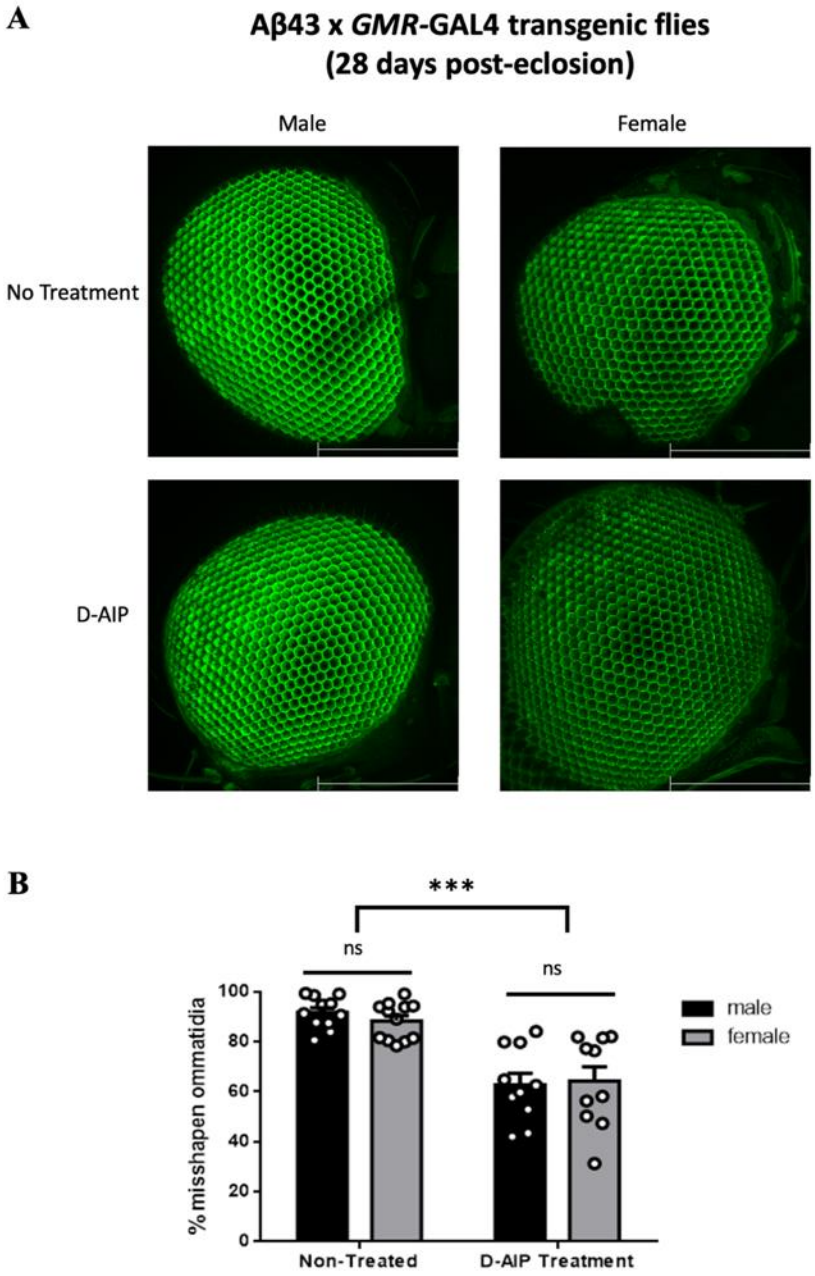

Figure 14. D-AIP treatment attenuates Aβ43-induced eye toxicity in transgenic flies at 28 days post-eclosion

A. Representative live confocal images of transgenic Aβ43-expressing *Drosophila melanogaster* compound eyes at 28 days post-eclosion, feeding on either regular or D-AIP supplemented food. Scale bar: 200μm. **B.** Quantification of percent of misshapen ommatidia. Kruskal-Wallis analyses were performed, revealing that D-AIP treatment significantly reduced the percent of misshapen ommatidia, ***$p < 0.001$. No significant effect of sex on eye toxicity was found, $p > 0.05$. Data is represented as mean ± SEM. Two to three flies were imaged per treatment replicate, n = 4.

4.8. D-AIP attenuates the Aβ42-induced toxic "rough eye" phenotype in transgenic *Drosophila melanogaster* only at five days post-eclosion

Analogous to Aβ43-expressing flies, transgenic *Drosophila melanogaster* with eye-specific expression of Aβ42 were bred and raised for 28 days on either D-AIP supplemented or non-supplemented food. Flies were separated by sex and their eye morphology was captured longitudinally using live confocal imaging over the 28-day treatment period. The eye-morphology of flies from each sex and treatment group were evaluated and their percent of misshapen ommatidia (toxic "rough eye" phenotype) were quantified at five, 14, and 28 days post-eclosion **(Figures 15-17)**. Non-parametric Kurskal-Wallis Tests were performed on quantification data from all three time points, due to unequal variances between groups (day five and day 14) or non-normal distribution of the data (day 28). There was a significant effect of D-AIP on the "rough eye" phenotype at five days post-eclosion, $H(1) = 4.671$, $p = 0.031$, where transgenic flies treated with D-AIP demonstrated a significantly lower median percent of misshapen ommatidia (median (female) = 88.89%, median (male) = 86.06%) compared to the non-treated group (median (female) = 94.76%, median (male) = 89.61%). However, at 14 and 28 days post-eclosion, D-AIP did not have a significant effect on the "rough eye" phenotype; the median percentage of misshapen ommatidia in the D-AIP treated group (day 14: median (female) = 92.31%, median (male) = 83.13%; day 28: median (female) = 95.78%, median (male) = 93.14%) was not significantly different than that of the non-treated group (day 14: median (female) = 95.88%, median (male) = 96.73%; day 28: median (female) = 94.75%, median (male) = 96.50%), day 14: $H(1) = 3.692$, $p = 0.055$; day 28: $H(1) = 0.070$, $p = 0.792$. There was no significant effect of sex on "rough eye" phenotype at five days post-eclosion, $H(1) = 2.628$, $p = 0.105$, 14 days post-eclosion, $H(1) = 0.410$, $p = 0.522$, or 28 days post-eclosion, $H(1) = 0.214$, $p = 0.644$.

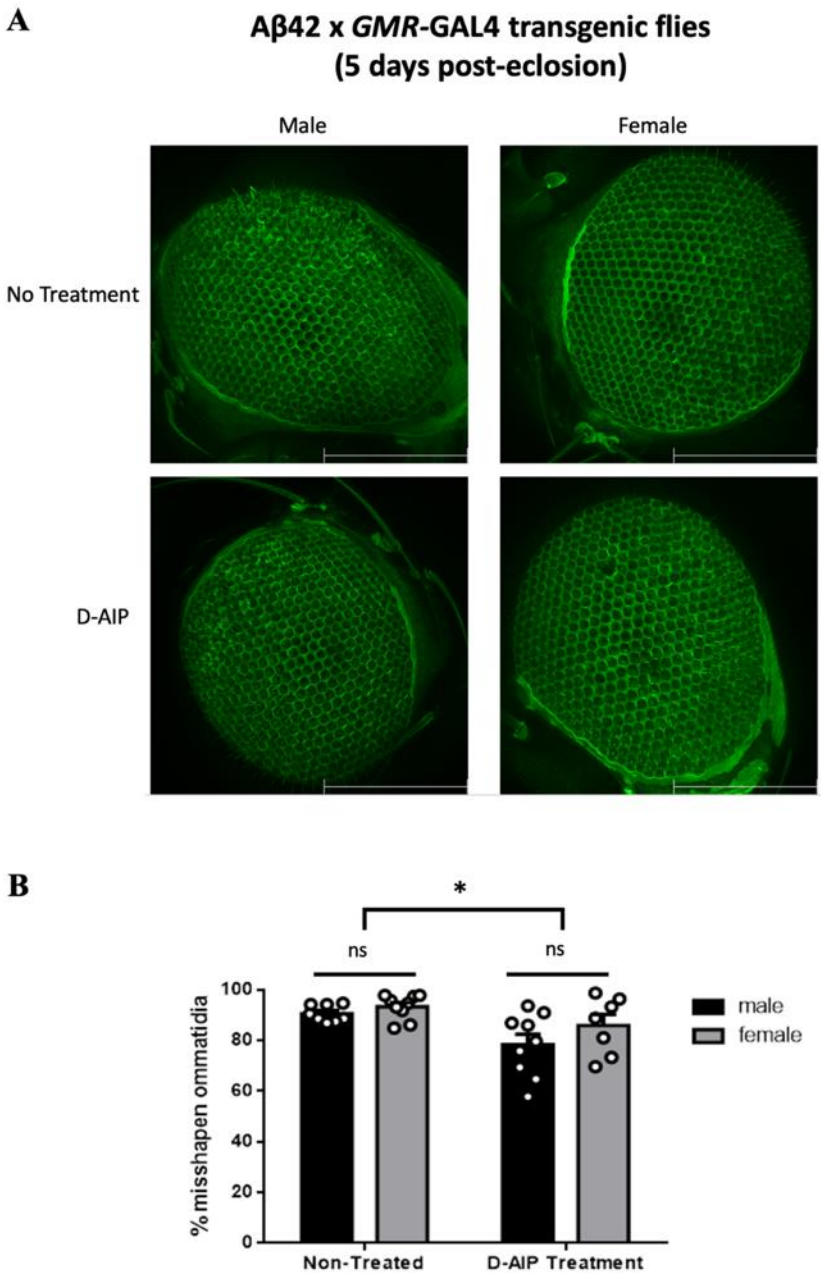

Figure 15. D-AIP treatment attenuates Aβ42-induced eye toxicity in transgenic flies at five days post-eclosion

A. Representative live confocal images of transgenic Aβ42-expressing *Drosophila melanogaster* compound eyes at five days post-eclosion, feeding on either regular or D-AIP supplemented food. Scale bar: 200μm. **B.** Quantification of percent of misshapen ommatidia. Kruskal-Wallis analyses were performed, revealing that D-AIP treatment significantly reduced the percent of misshapen ommatidia, $*p = 0.031$. No significant effect of sex on eye toxicity was found, $p > 0.05$. Data is represented as mean ± SEM. Two to three flies were imaged per treatment replicate, n = 3.

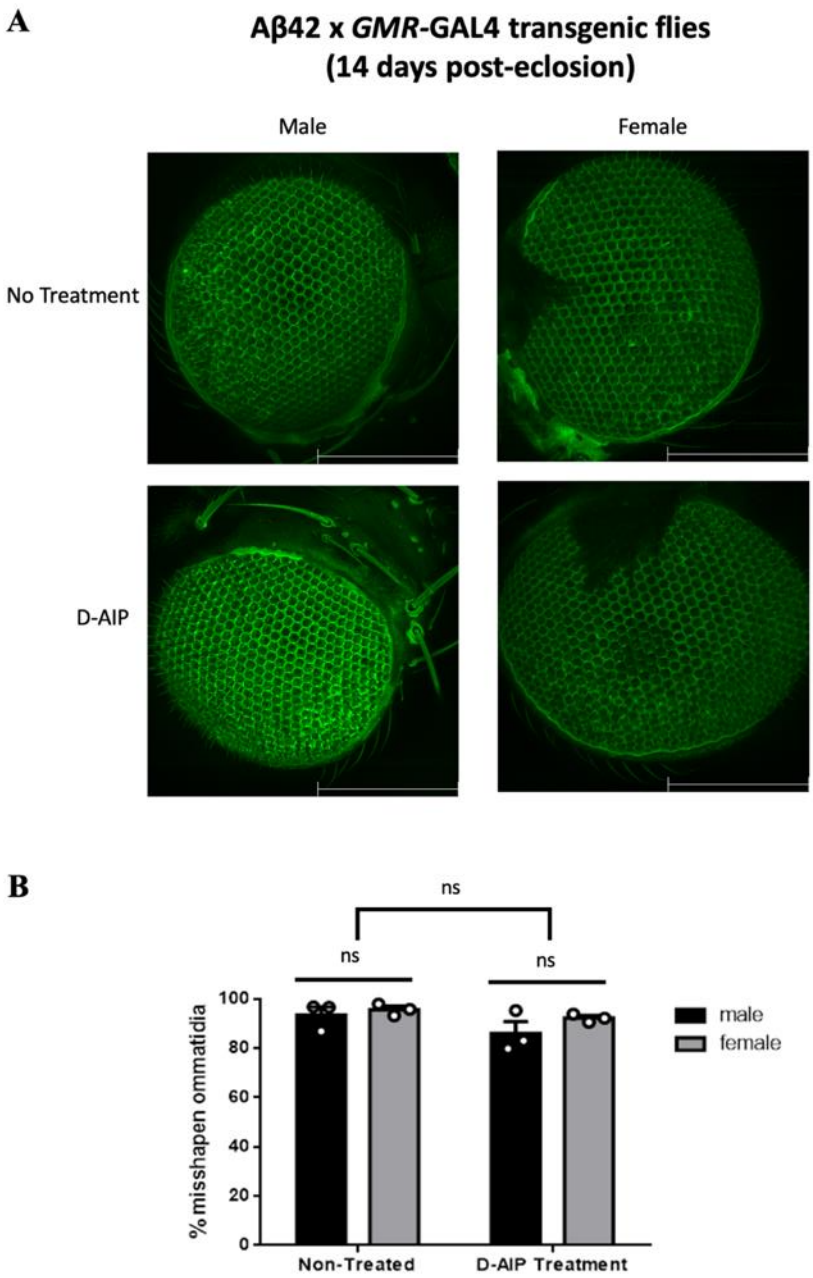

Figure 16. D-AIP treatment attenuates Aβ42-induced eye toxicity in transgenic flies at 14 days post-eclosion

A. Representative live confocal images of transgenic Aβ42-expressing *Drosophila melanogaster* compound eyes at five days post-eclosion, feeding on either regular or D-AIP supplemented food. Scale bar: 200μm. **B.** Quantification of percent of misshapen ommatidia. Kruskal-Wallis analyses were performed, revealing that D-AIP treatment did not significantly reduce the percent of misshapen ommatidia, $p = 0.055$. No significant effect of sex on eye toxicity was found, $p > 0.05$. Data is represented as mean ± SEM. One fly was imaged per treatment replicate, n = 3.

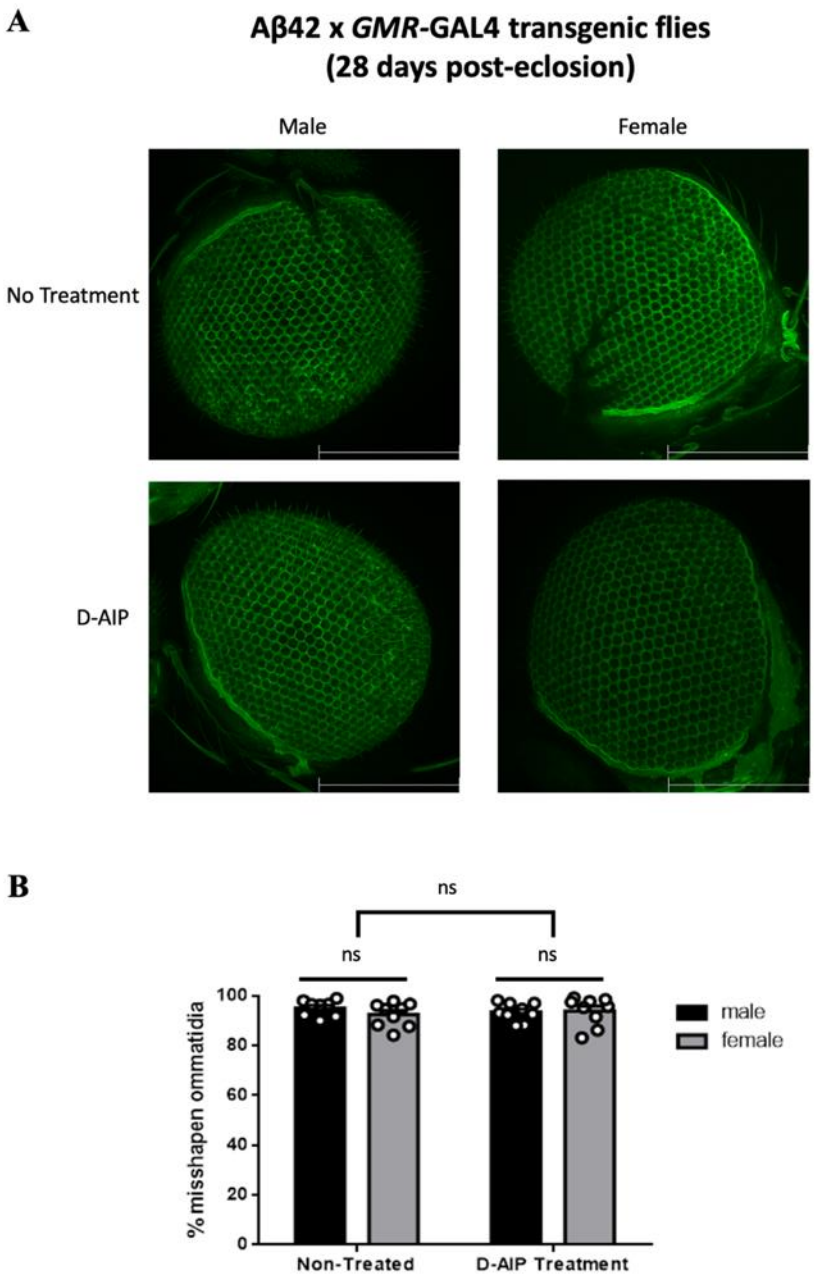

Figure 17. D-AIP treatment attenuates Aβ42-induced eye toxicity in transgenic flies at 28 days post-eclosion

A. Representative live confocal images of transgenic Aβ42-expressing *Drosophila melanogaster* compound eyes at five days post-eclosion, feeding on either regular or D-AIP supplemented food. Scale bar: 200μm. **B.** Quantification of percent of misshapen ommatidia. Kruskal-Wallis analyses were performed, revealing that D-AIP treatment did not significantly reduce the percent of misshapen ommatidia, $p = 0.792$. No significant effect of sex on eye toxicity was found, $p > 0.05$. Data is represented as mean ± SEM. Two to three flies were imaged per treatment replicate, n = 3.

DISCUSSION

The recently FDA-approved disease-modifying therapeutics for AD (aducanumab and lecanemab) are encouraging for the field – however, controversy surrounding the efficacy, cost, and safety profiles of these passive immunotherapies emphasizes the imminent need for novel therapeutic intervention strategies. The Multhaup lab has previously characterized an eight D-amino-acid peptide termed D-AIP, and demonstrated its ability *in vitro* and *in vivo* to interact with low-order oligomers of Aβ42, attenuate its toxicity, and disrupt its sheet-to-sheet packing, consequently blocking Aβ fibril formation[66,67,73]. While D-AIP was shown to interact with Aβ42, its ability to target other Aβ species has not yet been investigated. Considering the role of Aβ43 in AD and CAA (as a neurotoxic peptide and seeding agent for other Aβ species), the current study sought to investigate if D-AIP targets Aβ43 longitudinally *in vivo*. After characterizing a transgenic *Drosophila melanogaster* "rough eye" phenotype model induced by eye-directed expression of Aβ43, our longitudinal study found that D-AIP attenuated Aβ43-induced toxicity over a 28-day treatment period, with no sex-specific effects. We also validated our lab's previous findings on D-AIP's biostability, its ability to cross the invertebrate BBB, and that D-AIP does not produce negative side effects on the longevity of *Drosophila*.

5.1. Transgenic *Drosophila melanogaster* with eye-directed expression of Aβ43 constitutes as an appropriate model of toxicity

We aimed to use the transgenic *Drosophila melanogaster* "rough eye" phenotype as a model of Aβ toxicity. In contrast to the well-established Aβ42-induced "rough eye" *Drosophila* model that our lab utilized in the previous *in vivo* AIP studies, the Aβ43-induced "rough eye" model is less frequently studied or characterized. It was necessary to first characterize a transgenic Aβ43 *Drosophila* model and explore the level of toxicity ("rough eye" phenotype) induced by eye-

directed expression of Aβ43, to properly establish a baseline of toxicity in our model prior to conducting any therapeutic experiments.

After validating presence of the human Aβ43 transgene in the parental UAS-Aβ43 *Drosophila* strain, this strain was crossed with the *GMR*-GAL4 parental strain to induce eye-directed expression of human Aβ43. Immunoprecipitation and western blotting of the progeny successfully confirmed Aβ43 expression in their heads **(Figure 3)**. Upon verified expression of Aβ43, the toxicity induced by Aβ43 expression was investigated at 5 and 28 days post-eclosion, using live confocal imaging to examine compound eye morphology. Quantifications of eye morphology revealed that Aβ43 induces a toxic, "rough eye" phenotype in both males and females at 5 **(Figure 4)** and 28 days-post eclosion **(Figure 5)**, increasing in severity with age. Although these transgenic flies presented a "rough eye" phenotype, the severity was significantly lower than that induced by Aβ42 in transgenic *Drosophila*. This result aligns with previous literature on expression of Aβ43 in the eyes of *Drosophila melanogaster* relative to Aβ42 expression. In 2015, Burnouf et al. reported eye (*GMR*-driven) expression of Aβ43 to have a significantly toxic effect on the morphology of the compound eye in transgenic *Drosophila* – although they emphasized that the effect was significantly milder than the toxicity induced by the expression of Aβ42 in the eyes of transgenic flies[47]. Further, this result supports the *in vitro* findings of Barucker et al. (2014) that although Aβ43 and Aβ42 exhibited significant toxicity, Aβ42 reduced cell viability to a greater extent than Aβ43[78].

It is also important to note that the quantified toxic "rough eye" in *GMR*-GAL4 driver control flies was not at 0% severity, but was rather 18.4 ± 3.3% and 17.9 ± 2.5% for 5 days and 28 days post-eclosion, respectively. This result was expected, as the Wildtype Canton S. line (which does not possess a rough eye phenotype) was not being used – instead, our experiment used the

progeny of a cross between the Canton S. line and the *GMR*-GAL4 line to obtain a control for *GMR*-GAL4 driver effects in progeny. In agreement with literature on the methodology of assessing the rough-eye phenotype, *GMR*-GAL4 driver control flies are known to possess a mild "rough eye" phenotype on their own, and it is necessary analyze the phenotype of these flies as experimental controls, relative to experimental lines[71].

5.2. Detection and biostability of D-AIP in the heads and bodies of transgenic *Drosophila melanogaster*

Following characterization of the Aβ43 transgenic *Drosophila* model, we proceeded with experiments to analyze the effects of D-AIP food supplementation in this model. Flies were bred and raised for 28 days on either normal food or food supplemented with D-AIP. Following the treatment period, the presence of D-AIP in both the heads and bodies of treated flies was examined using MALDI mass spectrometry by Dr. Mark Hancock. The 941.477 *m/z* peak of D-AIP was detected in spectra of homogenates from the heads and bodies of flies treated with D-AIP, while the peak was absent in the spectra of flies from the non-treated groups **(Figures 7-8)**. The presence of D-AIP in the heads of treated flies indicate that D-AIP was consumed and was likely able to cross the invertebrate BBB. This finding is supported by the results of our previous study on D-AIP and Aβ42 in transgenic *Drosophila*, where D-AIP was detected in the heads of *Drosophila* by both MALDI mass spectrometry and MALDI mass spectrometry imaging (MSI)[67].

The peak of intact D-AIP in the MALDI mass spectrometry spectra of our current study also highlights the biostability and resistance to proteolysis of D-AIP *in vivo*, in line with our lab's previous *in vivo* study. Zhong et al. (2019) reported on the biostability of L-AIP compared to D-AIP in *Drosophila*, where L-AIP was rapidly degraded *in vivo*, compared to D-AIP which

remained intact. D-AIP's likely resistance to proteolysis and stability in *Drosophila melanogaster* is encouraging for future studies on D-AIP administration in higher order *in vivo* models.

The likelihood of the current study's detection of D-AIP in transgenic *Drosophila* being a result of contamination is extremely low. This is not only because of the analogous results in our lab's previous study and their specific localization of D-AIP by MALDI-MSI[67], but also because of our methods for handling the experimental flies prior to homogenization. To sanitize surfaces and prevent static electricity when separating flies into tubes for snap-freezing, surfaces were wiped down with 70% ethanol – further, all flies were handled with a small paintbrush which was freshly soaked in 70% ethanol. Consequently, as flies were separated into tubes for snap-freezing, they were fully coated in fresh ethanol; any residual D-AIP supplemented food which may have stuck to the flies would have been wiped away with each brush stroke of ethanol.

5.3. Levels of Aβ43 or Aβ42 in transgenic *Drosophila melanogaster* are not affected by D-AIP treatment

The expression of Aβ43 **(Figure 9A)** and Aβ42 **(Figure 10A)** was confirmed in 28-day-old experimental flies of both sexes from D-AIP treated and non-treated groups by immunoprecipitation and western blotting. To investigate if D-AIP affected Aβ levels after 28 days of treatment, relative levels of either PBS-soluble or GdnHCl-soluble Aβ43 were quantified from western blots of either D-AIP treated or non-treated flies from both sexes. In either sex, no significant changes in Aβ43 levels were detected between treated and non-treated groups **(Figure 9B)**. Likewise, no significant changes in levels Aβ42 were detected between treated and non-treated groups **(Figure 10B)**. Theoretically (for both Aβ43 or Aβ42), if D-AIP interacted with and "trapped" soluble low-order oligomers of Aβ and decreased subsequent fibril formation, one would expect soluble Aβ levels to increase and insoluble Aβ levels to decrease in D-AIP treated groups

relative to non-treated groups. Although statistically insignificant, this trend is visible in the quantifications of soluble Aβ43 in both females and males, and of insoluble Aβ43 in females **(Figure 9B)**. While no significant differences in Aβ43 or Aβ42 levels were observed between treated and non-treated groups, this result actually aligns with the results of our lab's previous study investigating D-AIP on Aβ42 in transgenic *Drosophila*[67]. Zhong et al. (2019) reported no significant differences in levels of Aβ42 in the heads of treated and non-treated flies, after performing quantifications on western blots of immunoprecipitated Aβ42. The previous 2019 study and this current study both used the same methodology to investigate relative levels of Aβ, which may now reveal a limitation in these experiments. A higher sensitivity assay, such as Meso Scale Discovery (MSD) immunoassay which has been utilized by other groups working with transgenic Aβ-expressing flies[77,79], would provide more precise and informative quantifications of Aβ levels.

In the quantifications of relative Aβ43 and Aβ42 in both soluble and insoluble fractions, a difference in relative Aβ levels is observed between males and females. In both fractions, male flies appear to present higher relative levels of Aβ43 and Aβ42, compared to female flies. This observation was unexpected, considering there were no sex-specific differences of eye toxicity in our initial characterization experiments. However unanticipated, Iijima et al. (2004) used the GAL4-UAS system to induce Aβ expression in *Drosophila* and observed increased expression of Aβ40 and Aβ42 in males relative to females. They reported the difference to be partially explained by gene dosage compensation, as the GAL4 promoter is located on the X chromosome[80], which may also be the source of differences in Aβ expression between sex in the current study.

5.4. D-AIP longitudinally attenuates Aβ43-induced eye toxicity, but only attenuates Aβ42-induced toxicity at day 5 post-eclosion in transgenic *Drosophila melanogaster*

Upon verification of D-AIP uptake and Aβ43 or Aβ42 expression in experimental transgenic Drosophila, their eye morphology was assessed and quantified at three time points during a 28-day treatment period using live confocal imaging.

D-AIP was found to significantly reduce the severity of Aβ43-induced toxic "rough eye" phenotype in male and female transgenic *Drosophila* at all three experimental time points. Interestingly, the mean quantifications of toxicity in D-AIP treated groups remained fairly consistent at all three time points, while the severity of eye toxicity of non-treated groups increased considerably between each time point as they aged **(Figures 12-14)**. Given the transgenic *Drosophila* were also bred on D-AIP, these results and observations indicate that D-AIP likely targeted and interacted with Aβ43 in the eyes of these *Drosophila* at a very young age, interfering with Aβ43's toxicity and aggregation. Given that Aβ43-induced toxicity in *Drosophila* increases with age[47], it is probable that D-AIP's early-age effect was necessary for the sustained attenuation of toxicity as the *Drosophila* aged – modeling the critical need to begin therapeutic interventions as close to the onset of AD or CAA pathology possible.

No sex-specific effects of D-AIP were observed at any time point in Aβ43 transgenic flies – however, there was a significant effect of sex on the severity of "rough eye" toxicity at 14 days post-eclosion **(Figure 13B)**. Although statistically significant, the effect of sex is most likely the result of a small sample size and not a true reflection of the population. This proposition becomes evident when comparing the number of replicates in the live confocal imaging groups at 14 days post-eclosion against the number of replicates from five and 28 days post-eclosion (where no effect

of sex was found). Further investigation with additional replicates at the 14-day post-eclosion time point would be necessary to properly assess the significant effect of sex found in the current study.

In contrast to the longitudinal effects of D-AIP observed in Aβ43 transgenic *Drosophila*, D-AIP was only found to attenuate the toxicity of Aβ42 in the eyes of transgenic *Drosophila* at five days post-eclosion **(Figure 15)**, but not at 14 or 28 days post-eclosion **(Figures 16-17)**. No sex-specific effects of D-AIP were found, and no effect of sex on the severity of eye toxicity were detected. The inclusion of Aβ42-expressing transgenic *Drosophila* in the current study were intended to serve as a control for an established model of Aβ-induced eye toxicity, while additionally investigating the reproducibility of our lab's previous findings from Zhong et al. (2019). The results from our current study on D-AIP in transgenic Aβ42 flies are similar (but not identical) to the results reported in our lab's previous longitudinal study on D-AIP in transgenic Aβ42 *Drosophila*[67]. Both the previous and our current studies found that D-AIP was able to attenuate the toxic "rough eye" phenotype induced by Aβ42 at five days post-eclosion, but not at 28 days post-eclosion. In the current study, an additional experimental time point was added at 14 days post-eclosion, however, D-AIP was still unable to attenuate Aβ42-induced toxicity at that time point **(Figure 16)**. The validation that D-AIP is only able to attenuate Aβ42 toxicity at an early time point, and not longitudinally, speaks to the high level of toxicity that the non-native human Aβ42 induces in *Drosophila* early-on. It is possible that the irreversible damage to photoreceptors and accessory cells (induced by extracellular secretion of human Aβ42) in *Drosophila* was already at such a high level at five days post-eclosion, that any intervention to slow or prevent future damage would present within such a small margin of difference which would not be detected by our current method.

The attenuation of Aβ42 toxicity at five days post-eclosion by D-AIP observed in the current study was not sex-specific, attenuating the toxicity in both males and females. This result is in contrast to the lab's previous study, which found that D-AIP only significantly attenuated Aβ42-induced toxicity in female flies[67]. Zhong et al. (2019) attributed the sex-specific effect of D-AIP as a confounding factor, due to the accessory gland protein-70A (Acp70A), a male-specific sex peptide in *Drosophila* which was found to co-localize with D-AIP in the gut[67]. As no sex-specific effects of D-AIP were found in the current study, it brings into question a possible weakness of the methods of quantification. In both the current and previous study on D-AIP and Aβ42, assessment and quantification of eye toxicity severity was performed by a single observer. Although in line with guidelines by Giannakou and Crowther (2011) which state that assessment of the "rough eye" phenotype should be carried out by a single observer, the authors also emphasized that "rough eye" phenotype assessments are intended to be qualitative[71]; naturally, with no inter-rater reliability or standardized method of assessment between studies, variability in results is bound to occur. Future therapeutic screening experiments utilizing the "rough eye" phenotype in *Drosophila* would benefit from alternative standardized assessment/quantification methods, such as the automated Flynotyper software[81].

This study demonstrated the variance of D-AIP's capacity to longitudinally attenuate different Aβ species *in vivo*. While Aβ43-induced toxicity was attenuated for the duration of a 28-day treatment period, D-AIP did not attenuate Aβ42 toxicity at the time points beyond five days post-eclosion. As the interactions of D-AIP with Aβ42[66] or Aβ43 (Shobo and Sarty et al., unpublished) have each been confirmed by test tube incubation experiments in our lab, we suspect the differential attenuation results to be associated with levels of soluble oligomeric forms of Aβ43 or Aβ42 which induce eye toxicity. Our Western blot quantifications showed considerably higher

levels of soluble Aβ43 **(Figure 9)** than Aβ42 **(Figure 10)**, demonstrating the differences between Aβ43 and Aβ42 in both their aggregation behaviour and consequent levels of oligomers. The increased presence of soluble Aβ43 could be attributed to the speed of Aβ43 or Aβ42 aggregation; Aβ42 may aggregate more rapidly than Aβ43, causing only a brief period that D-AIP may be effective at targeting Aβ42 oligomers. It would be reasonable to infer that Aβ43 oligomers may have been present for a longer time than Aβ42 oligomers, allowing D-AIP target Aβ43 oligomers over a longer duration. However, it should be noted that aggregation speed of Aβ43 relative to Aβ42 remains somewhat of a contradicting topic in the literature. While Chemuru et al. (2016) found that Aβ43 aggregates more slowly than Aβ42[82], Saito et al. (2011) observed increased aggregation propensity of Aβ43 compared to Aβ42[41]. Moreover, other studies have found no difference between Aβ43 and Aβ42 aggregation kinetics[48,83,84]. In agreement with our lab's previous study investigating properties of synthetic Aβ42 peptides[85], variation in these observations is most likely due to the use of differentially sourced Aβ peptides and their varied concentrations used in experimental approaches. Future studies on relative concentrations of Aβ43 or Aβ42 oligomers at a given point in time *in vivo* are necessary to further our understanding the difference in D-AIP's targeting of Aβ43 and Aβ42 toxicity.

5.5. Future investigation of D-AIP in transgenic *Drosophila melanogaster* and higher order *in vivo* models

The use of *Drosophila melanogaster* as a therapeutic screening model has been extremely beneficial in our lab's D-AIP studies. Although *Drosophila melanogaster* have an APP ortholog (APPL), the Aβ-encoding region of APPL is not conserved, so they do not endogenously express Aβ peptides[86,87]. The lack of endogenous Aβ expression consequently allows for controlled screening studies, in which D-AIP's efficacy of targeting a specific Aβ species can be carried out

in a transgenic *Drosophila* model expressing a given species of human Aβ. It would be of interest to investigate the effect of D-AIP on Aβ43 seeding in a transgenic *Drosophila melanogaster* model which co-expresses multiple human Aβ species. Burnouf et al. (2015) characterized a transgenic *Drosophila* model which co-express Aβ43 and Aβ40 pan-neuronally; the expression of Aβ43 was found to induce toxicity and aggregation of the normally non-toxic and non-aggregating Aβ40, resulting in synergistic toxic effects on climbing ability and lifespan these flies[47]. The investigation of D-AIP's effect on Aβ43 seeding in this *Drosophila* model would be of value moving forward.

Moving beyond therapeutic screening studies, it is useful to utilize higher-order *in vivo* AD or CAA models, which possess more complex and/or mixed Aβ pathology. Based on the results of our current study, where D-AIP was found to affect both Aβ43 and Aβ42 toxicity to different extents, it would be beneficial to further investigate the effect of D-AIP on AD/CAA pathology in a more complex model. Future studies may employ the ArcAβ mouse model, which express human APP with combined Arctic (E693G) and Swedish (K670N/M671L) mutations, leading to the development of Aβ pathology in brain parenchyma and vasculature, and cognitive impairments[88]. It would be imperative to longitudinally assess the ability of D-AIP to not only reduce the differentially localized Aβ pathology, but to also evaluate if D-AIP can rescue impaired cognition in these transgenic mice.

5. CONCLUSION

The results of this thesis have demonstrated that D-AIP can target and longitudinally attenuate Aβ43-induced toxicity in transgenic *Drosophila melanogaster* and have validated our lab's previous findings that D-AIP attenuates Aβ42-induced toxicity only at the five days post-eclosion point in transgenic *Drosophila*. This study successfully characterized a transgenic *Drosophila* model with eye-directed expression of Aβ43 for its use in subsequent D-AIP therapeutic screening studies. D-AIP was confirmed as biostable *in vivo* and produced no negative side effects on the longevity of transgenic *Drosophila melanogaster*. Together, as D-AIP was found to target two key Aβ peptides heavily involved in the pathology of both AD and CAA, the results of this study suggest that D-AIP presents as a promising therapeutic candidate to prevent or delay the progression of AD and/or CAA. Moving forward, it would be valuable to study the effect of D-AIP on Aβ43 seeding in transgenic *Drosophila* models of mixed Aβ43 and Aβ40 expression, and in more complex rodent models of AD and CAA pathologies.

7. REFERENCES

1 2022 Alzheimer's disease facts and figures. *Alzheimer's & Dementia* **18**, 700-789 (2022). https://doi.org:https://doi.org/10.1002/alz.12638

2 Maurer, K., Volk, S. & Gerbaldo, H. Auguste D and Alzheimer's disease. *The Lancet* **349**, 1546-1549 (1997). https://doi.org:10.1016/S0140-6736(96)10203-8

3 Stelzmann, R. A., Norman Schnitzlein, H. & Reed Murtagh, F. An english translation of alzheimer's 1907 paper, "über eine eigenartige erkankung der hirnrinde". *Clinical Anatomy* **8**, 429-431 (1995). https://doi.org:https://doi.org/10.1002/ca.980080612

4 Katzman, R. The Prevalence and Malignancy of Alzheimer Disease: A Major Killer. *Archives of Neurology* **33**, 217-218 (1976). https://doi.org:10.1001/archneur.1976.00500040001001

5 Lane, C. A., Hardy, J. & Schott, J. M. Alzheimer's disease. *European Journal of Neurology* **25**, 59-70 (2018). https://doi.org:https://doi.org/10.1111/ene.13439

6 Lacorte, E. *et al.* Safety and Efficacy of Monoclonal Antibodies for Alzheimer's Disease: A Systematic Review and Meta-Analysis of Published and Unpublished Clinical Trials. *Journal of Alzheimer's Disease* **87**, 101-129 (2022). https://doi.org:10.3233/JAD-220046

7 Reardon, S. FDA approves Alzheimer's drug lecanemab amid safety concerns. *Nature* **613**, 227-228 (2023). https://doi.org:10.1038/d41586-023-00030-3

8 Hyman, B. T. *et al.* National Institute on Aging-Alzheimer's Association guidelines for the neuropathologic assessment of Alzheimer's disease. *Alzheimers Dement* **8**, 1-13 (2012). https://doi.org:10.1016/j.jalz.2011.10.007

9 Trejo-Lopez, J. A., Yachnis, A. T. & Prokop, S. Neuropathology of Alzheimer's Disease. *Neurotherapeutics* **19**, 173-185 (2022). https://doi.org:10.1007/s13311-021-01146-y

10 Jack, C. R. *et al.* Hypothetical model of dynamic biomarkers of the Alzheimer's pathological cascade. *The Lancet Neurology* **9**, 119-128 (2010). https://doi.org:https://doi.org/10.1016/S1474-4422(09)70299-6

11 Haass, C. & Selkoe, D. J. Soluble protein oligomers in neurodegeneration: lessons from the Alzheimer's amyloid β-peptide. *Nature reviews Molecular cell biology* **8**, 101-112 (2007).

12 Van Cauwenberghe, C., Van Broeckhoven, C. & Sleegers, K. The genetic landscape of Alzheimer disease: clinical implications and perspectives. *Genet Med* **18**, 421-430 (2016). https://doi.org:10.1038/gim.2015.117

13 Piaceri, I., Nacmias, B. & Sorbi, S. Genetics of familial and sporadic Alzheimer's disease. *FBE* **5**, 167-177 (2013). https://doi.org:10.2741/e605

14 Olloquequi, J. *et al.* Impact of New Drugs for Therapeutic Intervention in Alzheimer's Disease. *FBL* **27** (2022). https://doi.org:10.31083/j.fbl2705146

15 Hardy, J. Amyloid, the presenilins and Alzheimer's disease. *Trends in Neurosciences* **20**, 154-159 (1997). https://doi.org:https://doi.org/10.1016/S0166-2236(96)01030-2

16 Prüßing, K., Voigt, A. & Schulz, J. B. Drosophila melanogaster as a model organism for Alzheimer's disease. *Molecular Neurodegeneration* **8**, 35 (2013). https://doi.org:10.1186/1750-1326-8-35

17 Selkoe, D. J. & Hardy, J. The amyloid hypothesis of Alzheimer's disease at 25 years. *EMBO Molecular Medicine* **8**, 595-608 (2016). https://doi.org:https://doi.org/10.15252/emmm.201606210

18 Olsson, F. *et al.* Characterization of intermediate steps in amyloid beta (Aβ) production under near-native conditions. *J Biol Chem* **289**, 1540-1550 (2014). https://doi.org:10.1074/jbc.M113.498246
19 Wiseman, F. K. *et al.* A genetic cause of Alzheimer disease: mechanistic insights from Down syndrome. *Nature Reviews Neuroscience* **16**, 564-574 (2015). https://doi.org:10.1038/nrn3983
20 Glenner, G. G. & Wong, C. W. Alzheimer's disease and Down's syndrome: Sharing of a unique cerebrovascular amyloid fibril protein. *Biochemical and Biophysical Research Communications* **122**, 1131-1135 (1984). https://doi.org:https://doi.org/10.1016/0006-291X(84)91209-9
21 Postina, R. Activation of α-secretase cleavage. *Journal of Neurochemistry* **120**, 46-54 (2012). https://doi.org:https://doi.org/10.1111/j.1471-4159.2011.07459.x
22 Zhang, Y.-w., Thompson, R., Zhang, H. & Xu, H. APP processing in Alzheimer's disease. *Molecular Brain* **4**, 3 (2011). https://doi.org:10.1186/1756-6606-4-3
23 Tan, F. H. P. & Azzam, G. Drosophila melanogaster: Deciphering Alzheimer's Disease. *Malays J Med Sci* **24**, 6-20 (2017). https://doi.org:10.21315/mjms2017.24.2.2
24 Wang, X. *et al.* Modifications and Trafficking of APP in the Pathogenesis of Alzheimer's Disease. *Frontiers in Molecular Neuroscience* **10** (2017). https://doi.org:10.3389/fnmol.2017.00294
25 Skovronsky, D. M., Moore, D. B., Milla, M. E., Doms, R. W. & Lee, V. M. Y. Protein Kinase C-dependent α-Secretase Competes with β-Secretase for Cleavage of Amyloid-β Precursor Protein in the Trans-Golgi Network*. *Journal of Biological Chemistry* **275**, 2568-2575 (2000). https://doi.org:https://doi.org/10.1074/jbc.275.4.2568
26 Sannerud, R. *et al.* Restricted Location of PSEN2/γ-Secretase Determines Substrate Specificity and Generates an Intracellular Aβ Pool. *Cell* **166**, 193-208 (2016). https://doi.org:https://doi.org/10.1016/j.cell.2016.05.020
27 Nikolaev, A., McLaughlin, T., O'Leary, D. D. M. & Tessier-Lavigne, M. APP binds DR6 to trigger axon pruning and neuron death via distinct caspases. *Nature* **457**, 981-989 (2009). https://doi.org:10.1038/nature07767
28 Kimura, A., Hata, S. & Suzuki, T. Alternative Selection of β-Site APP-Cleaving Enzyme 1 (BACE1) Cleavage Sites in Amyloid β-Protein Precursor (APP) Harboring Protective and Pathogenic Mutations within the Aβ Sequence. *J Biol Chem* **291**, 24041-24053 (2016). https://doi.org:10.1074/jbc.M116.744722
29 Serrano-Pozo, A., Frosch, M. P., Masliah, E. & Hyman, B. T. Neuropathological alterations in Alzheimer disease. *Cold Spring Harb Perspect Med* **1**, a006189 (2011). https://doi.org:10.1101/cshperspect.a006189
30 Jellinger, K. A. Alzheimer disease and cerebrovascular pathology: an update. *Journal of Neural Transmission* **109**, 813-836 (2002). https://doi.org:10.1007/s007020200068
31 Jäkel, L., Boche, D., Nicoll, J. A. R. & Verbeek, M. M. Aβ43 in human Alzheimer's disease: effects of active Aβ42 immunization. *Acta Neuropathologica Communications* **7**, 141 (2019). https://doi.org:10.1186/s40478-019-0791-6
32 Greenberg, S. M. *et al.* Cerebral amyloid angiopathy and Alzheimer disease—one peptide, two pathways. *Nature Reviews Neurology* **16**, 30-42 (2020).
33 Miller, D. L. *et al.* Peptide Compositions of the Cerebrovascular and Senile Plaque Core Amyloid Deposits of Alzheimer's Disease. *Archives of Biochemistry and Biophysics* **301**, 41-52 (1993). https://doi.org:https://doi.org/10.1006/abbi.1993.1112

34 Gravina, S. A. *et al.* Amyloid beta protein (A beta) in Alzheimer's disease brain. Biochemical and immunocytochemical analysis with antibodies specific for forms ending at A beta 40 or A beta 42(43). *J Biol Chem* **270**, 7013-7016 (1995). https://doi.org:10.1074/jbc.270.13.7013

35 Jan, A., Gokce, O., Luthi-Carter, R. & Lashuel, H. A. The ratio of monomeric to aggregated forms of Abeta40 and Abeta42 is an important determinant of amyloid-beta aggregation, fibrillogenesis, and toxicity. *J Biol Chem* **283**, 28176-28189 (2008). https://doi.org:10.1074/jbc.M803159200

36 Burdick, D. *et al.* Assembly and aggregation properties of synthetic Alzheimer's A4/beta amyloid peptide analogs. *Journal of Biological Chemistry* **267**, 546-554 (1992). https://doi.org:10.1016/S0021-9258(18)48529-8

37 Mann, D. M. *et al.* Predominant deposition of amyloid-beta 42(43) in plaques in cases of Alzheimer's disease and hereditary cerebral hemorrhage associated with mutations in the amyloid precursor protein gene. *Am J Pathol* **148**, 1257-1266 (1996).

38 Kakuda, N. *et al.* Distinct deposition of amyloid-β species in brains with Alzheimer's disease pathology visualized with MALDI imaging mass spectrometry. *Acta Neuropathol Commun* **5**, 73 (2017). https://doi.org:10.1186/s40478-017-0477-x

39 Akiyama, H. *et al.* Variable deposition of amyloid beta-protein (A beta) with the carboxy-terminus that ends at residue valine40 (A beta 40) in the cerebral cortex of patients with Alzheimer's disease: a double-labeling immunohistochemical study with antibodies specific for A beta 40 and the A beta that ends at residues alanine42/threonine43 (A beta 42). *Neurochem Res* **22**, 1499-1506 (1997). https://doi.org:10.1023/a:1021910729963

40 Jarrett, J. T., Berger, E. P. & Lansbury Jr, P. T. The carboxy terminus of the. beta. amyloid protein is critical for the seeding of amyloid formation: Implications for the pathogenesis of Alzheimer's disease. *Biochemistry* **32**, 4693-4697 (1993).

41 Saito, T. *et al.* Potent amyloidogenicity and pathogenicity of Aβ43. *Nature Neuroscience* **14**, 1023-1032 (2011). https://doi.org:10.1038/nn.2858

42 Benilova, I., Karran, E. & De Strooper, B. The toxic Aβ oligomer and Alzheimer's disease: an emperor in need of clothes. *Nature Neuroscience* **15**, 349-357 (2012). https://doi.org:10.1038/nn.3028

43 Conicella, A. E. & Fawzi, N. L. The C-Terminal Threonine of Aβ43 Nucleates Toxic Aggregation via Structural and Dynamical Changes in Monomers and Protofibrils. *Biochemistry* **53**, 3095-3105 (2014). https://doi.org:10.1021/bi500131a

44 Benilova, I. & De Strooper, B. An overlooked neurotoxic species in Alzheimer's disease. *Nature neuroscience* **14**, 949-950 (2011).

45 Ruiz-Riquelme, A. *et al.* Aβ43 aggregates exhibit enhanced prion-like seeding activity in mice. *Acta Neuropathologica Communications* **9**, 83 (2021). https://doi.org:10.1186/s40478-021-01187-6

46 Sandebring, A., Welander, H., Winblad, B., Graff, C. & Tjernberg, L. O. The Pathogenic Aβ43 Is Enriched in Familial and Sporadic Alzheimer Disease. *PLOS ONE* **8**, e55847 (2013). https://doi.org:10.1371/journal.pone.0055847

47 Burnouf, S., Gorsky, M. K., Dols, J., Grönke, S. & Partridge, L. Aβ43 is neurotoxic and primes aggregation of Aβ40 in vivo. *Acta Neuropathologica* **130**, 35-47 (2015). https://doi.org:10.1007/s00401-015-1419-y

48 Welander, H. *et al.* Aβ43 is more frequent than Aβ40 in amyloid plaque cores from Alzheimer disease brains. *Journal of Neurochemistry* **110**, 697-706 (2009). https://doi.org:https://doi.org/10.1111/j.1471-4159.2009.06170.x
49 Riek, R. & Eisenberg, D. S. The activities of amyloids from a structural perspective. *Nature* **539**, 227-235 (2016). https://doi.org:10.1038/nature20416
50 Biancalana, M. & Koide, S. Molecular mechanism of Thioflavin-T binding to amyloid fibrils. *Biochimica et Biophysica Acta (BBA) - Proteins and Proteomics* **1804**, 1405-1412 (2010). https://doi.org:https://doi.org/10.1016/j.bbapap.2010.04.001
51 Cohen, S. I. A. *et al.* Proliferation of amyloid-β42 aggregates occurs through a secondary nucleation mechanism. *Proceedings of the National Academy of Sciences* **110**, 9758-9763 (2013). https://doi.org:doi:10.1073/pnas.1218402110
52 Chatani, E. & Yamamoto, N. Recent progress on understanding the mechanisms of amyloid nucleation. *Biophysical Reviews* **10**, 527-534 (2018). https://doi.org:10.1007/s12551-017-0353-8
53 Törnquist, M. *et al.* Secondary nucleation in amyloid formation. *Chemical Communications* **54**, 8667-8684 (2018). https://doi.org:10.1039/C8CC02204F
54 McLean, C. A. *et al.* Soluble pool of Aβ amyloid as a determinant of severity of neurodegeneration in Alzheimer's disease. *Annals of Neurology* **46**, 860-866 (1999). https://doi.org:https://doi.org/10.1002/1531-8249(199912)46:6<860::AID-ANA8>3.0.CO;2-M
55 Abedini, A. *et al.* Time-resolved studies define the nature of toxic IAPP intermediates, providing insight for anti-amyloidosis therapeutics. *eLife* **5**, e12977 (2016). https://doi.org:10.7554/eLife.12977
56 Karran, E. & De Strooper, B. The amyloid hypothesis in Alzheimer disease: new insights from new therapeutics. *Nat Rev Drug Discov* **21**, 306-318 (2022). https://doi.org:10.1038/s41573-022-00391-w
57 Xie, Y. *et al.* Novel strategies for the fight of Alzheimer's disease targeting amyloid-β protein. *Journal of Drug Targeting* **30**, 259-268 (2022). https://doi.org:10.1080/1061186X.2021.1973482
58 Yiannopoulou, K. G. & Papageorgiou, S. G. Current and Future Treatments in Alzheimer Disease: An Update. *J Cent Nerv Syst Dis* **12**, 1179573520907397 (2020). https://doi.org:10.1177/1179573520907397
59 Hardy, J. & Selkoe, D. J. The amyloid hypothesis of Alzheimer's disease: progress and problems on the road to therapeutics. *Science* **297**, 353-356 (2002). https://doi.org:10.1126/science.1072994
60 Dhillon, S. Aducanumab: First Approval. *Drugs* **81**, 1437-1443 (2021). https://doi.org:10.1007/s40265-021-01569-z
61 Shi, M., Chu, F., Zhu, F. & Zhu, J. Impact of Anti-amyloid-β Monoclonal Antibodies on the Pathology and Clinical Profile of Alzheimer's Disease: A Focus on Aducanumab and Lecanemab. *Front Aging Neurosci* **14**, 870517 (2022). https://doi.org:10.3389/fnagi.2022.870517
62 Liu, W. *et al.* Structural Role of Glycine in Amyloid Fibrils Formed from Transmembrane α-Helices. *Biochemistry* **44**, 3591-3597 (2005). https://doi.org:10.1021/bi047827g
63 Harmeier, A. *et al.* Role of Amyloid-β Glycine 33 in Oligomerization, Toxicity, and Neuronal Plasticity. *The Journal of Neuroscience* **29**, 7582-7590 (2009). https://doi.org:10.1523/jneurosci.1336-09.2009

64 Munter, L. M. *et al.* GxxxG motifs within the amyloid precursor protein transmembrane sequence are critical for the etiology of Abeta42. *Embo j* **26**, 1702-1712 (2007). https://doi.org:10.1038/sj.emboj.7601616
65 Sato, T. *et al.* Inhibitors of amyloid toxicity based on beta-sheet packing of Abeta40 and Abeta42. *Biochemistry* **45**, 5503-5516 (2006). https://doi.org:10.1021/bi052485f
66 Barucker, C. *et al.* Aβ42-oligomer Interacting Peptide (AIP) neutralizes toxic amyloid-β42 species and protects synaptic structure and function. *Sci Rep* **5**, 15410 (2015). https://doi.org:10.1038/srep15410
67 Zhong, Y., Shobo, A., Hancock, M. A. & Multhaup, G. Label-free distribution of anti-amyloid D-AIP in Drosophila melanogaster: prevention of Aβ42-induced toxicity without side effects in transgenic flies. *Journal of Neurochemistry* **150**, 74-87 (2019). https://doi.org:https://doi.org/10.1111/jnc.14720
68 Feng, Z. & Xu, B. Inspiration from the mirror: D-amino acid containing peptides in biomedical approaches. *Biomol Concepts* **7**, 179-187 (2016). https://doi.org:10.1515/bmc-2015-0035
69 Pandey, U. B. & Nichols, C. D. Human disease models in Drosophila melanogaster and the role of the fly in therapeutic drug discovery. *Pharmacol Rev* **63**, 411-436 (2011). https://doi.org:10.1124/pr.110.003293
70 Stork, T. *et al.* Organization and function of the blood-brain barrier in Drosophila. *J Neurosci* **28**, 587-597 (2008). https://doi.org:10.1523/jneurosci.4367-07.2008
71 Giannakou, M. & Crowther, D. Vol. 48 223-240 (2011).
72 Pichaud, F. & Desplan, C. A new visualization approach for identifying mutations that affect differentiation and organization of the Drosophila ommatidia. *Development (Cambridge, England)* **128**, 815-826 (2001). https://doi.org:10.1242/dev.128.6.815
73 Shobo, A. *et al.* The amyloid-β1–42-oligomer interacting peptide D-AIP possesses favorable biostability, pharmacokinetics, and brain region distribution. *Journal of Biological Chemistry* **298** (2022). https://doi.org:10.1016/j.jbc.2021.101483
74 Brand, A. H. & Perrimon, N. Targeted gene expression as a means of altering cell fates and generating dominant phenotypes. *Development* **118**, 401-415 (1993). https://doi.org:10.1242/dev.118.2.401
75 Dourlen, P., Levet, C., Mejat, A., Gambis, A. & Mollereau, B. The Tomato/GFP-FLP/FRT method for live imaging of mosaic adult Drosophila photoreceptor cells. *J Vis Exp*, e50610 (2013). https://doi.org:10.3791/50610
76 Helmfors, L. *et al.* Protective properties of lysozyme on β-amyloid pathology: implications for Alzheimer disease. *Neurobiol Dis* **83**, 122-133 (2015). https://doi.org:10.1016/j.nbd.2015.08.024
77 Caesar, I., Jonson, M., Nilsson, K. P., Thor, S. & Hammarström, P. Curcumin promotes A-beta fibrillation and reduces neurotoxicity in transgenic Drosophila. *PLoS One* **7**, e31424 (2012). https://doi.org:10.1371/journal.pone.0031424
78 Barucker, C. *et al.* Nuclear translocation uncovers the amyloid peptide Aβ42 as a regulator of gene transcription. *J Biol Chem* **289**, 20182-20191 (2014). https://doi.org:10.1074/jbc.M114.564690
79 Jonson, M., Pokrzywa, M., Starkenberg, A., Hammarstrom, P. & Thor, S. Systematic Aβ Analysis in Drosophila Reveals High Toxicity for the 1-42, 3-42 and 11-42 Peptides, and Emphasizes N- and C-Terminal Residues. *PLOS ONE* **10**, e0133272 (2015). https://doi.org:10.1371/journal.pone.0133272

80 Iijima, K. *et al.* Dissecting the pathological effects of human Aβ40 and Aβ42 in Drosophila: A potential model for Alzheimer's disease. *Proceedings of the National Academy of Sciences* **101**, 6623-6628 (2004). https://doi.org:10.1073/pnas.0400895101

81 Iyer, J. *et al.* Quantitative Assessment of Eye Phenotypes for Functional Genetic Studies Using Drosophila melanogaster. *G3 (Bethesda)* **6**, 1427-1437 (2016). https://doi.org:10.1534/g3.116.027060

82 Chemuru, S., Kodali, R. & Wetzel, R. C-Terminal Threonine Reduces Aβ43 Amyloidogenicity Compared with Aβ42. *Journal of Molecular Biology* **428**, 274-291 (2016). https://doi.org:https://doi.org/10.1016/j.jmb.2015.06.008

83 Vandersteen, A. *et al.* A comparative analysis of the aggregation behavior of amyloid-β peptide variants. *FEBS Letters* **586**, 4088-4093 (2012). https://doi.org:https://doi.org/10.1016/j.febslet.2012.10.022

84 Jäkel, L., Biemans, E., Klijn, C. J. M., Kuiperij, H. B. & Verbeek, M. M. Reduced Influence of apoE on Aβ43 Aggregation and Reduced Vascular Aβ43 Toxicity as Compared with Aβ40 and Aβ42. *Mol Neurobiol* **57**, 2131-2141 (2020). https://doi.org:10.1007/s12035-020-01873-x

85 Shobo, A., Röntgen, A., Hancock, M. A. & Multhaup, G. Biophysical characterization as a tool to predict amyloidogenic and toxic properties of amyloid-β42 peptides. *FEBS Letters* **596**, 1401-1411 (2022). https://doi.org:https://doi.org/10.1002/1873-3468.14358

86 Rosen, D. R., Martin-Morris, L., Luo, L. Q. & White, K. A Drosophila gene encoding a protein resembling the human beta-amyloid protein precursor. *Proc Natl Acad Sci U S A* **86**, 2478-2482 (1989). https://doi.org:10.1073/pnas.86.7.2478

87 Luo, L., Tully, T. & White, K. Human amyloid precursor protein ameliorates behavioral deficit of flies deleted for appl gene. *Neuron* **9**, 595-605 (1992). https://doi.org:https://doi.org/10.1016/0896-6273(92)90024-8

88 Knobloch, M., Konietzko, U., Krebs, D. C. & Nitsch, R. M. Intracellular Abeta and cognitive deficits precede beta-amyloid deposition in transgenic arcAbeta mice. *Neurobiol Aging* **28**, 1297-1306 (2007). https://doi.org:10.1016/j.neurobiolaging.2006.06.019